FAA WJH Technical Center
00092809

CT
85
2

DOT/FAA/CT-85/2

Wall Flames and Implications for Upward Flame Spread

J. Quintiere (NBS)
M. Harkleroad (NBS)
Y. Hasemi (BRI, Japan)

Department of Commerce
National Bureau of Standards
Gaithersburg, Maryland

June 1985

Final Report

This document is available to the U.S. public through the National Technical Information Service, Springfield, Virginia 22161.

U.S. Department of Transportation
Federal Aviation Administration
Technical Center
Atlantic City Airport, N.J. 08405

NOTICE

This document is disseminated under the sponsorship of the Department of Transportation in the interest of information exchange. The United States Government assumes no liability for the contents or use thereof.

The United States Government does not endorse products or manufacturers. Trade or manufacturer's names appear herein solely because they are considered essential to the object of this report.

Technical Report Documentation Page

1. Report No. DOT/FAA/CT-85/2	2. Government Accession No.	3. Recipient's Catalog No.
4. Title and Subtitle Wall Flames and Implications for Upward Flame Spread		5. Report Date June 1985
		6. Performing Organization Code
7. Author(s) J. Quintiere, M. Harkleroad, Y. Hasemi		8. Performing Organization Report No.
9. Performing Organization Name and Address Department of Commerce National Bureau of Standards Bldg 224, Room A-345 Gaithersburg, Maryland 20899		10. Work Unit No. (TRAIS)
		11. Contract or Grant No.
12. Sponsoring Agency Name and Address U.S. Department of Transportation Federal Aviation Administration Technical Center Atlantic City Airport, New Jersey 08405		13. Type of Report and Period Covered
		14. Sponsoring Agency Code

15. Supplementary Notes

16. Abstract

This is a final report dealing with new concepts for predicting the flame spread on materials from laboratory measurements. It focuses on heat transfer which precipitates and precedes upward flame spread on a vertical surface. Six materials have been featured in this study as well as in past related studies. Their relevant flame spread measurements are presented. In this particular study heat transfer and flame height results are presented for wall samples burned at varying levels of external irradiance. Also complementary results are presented for methane line burner wall fires. An approximate theoretical analysis is included to serve as a guide to identifying the important variables and their relationship for correlation purposes. Experimental results yield flame height proportional to energy release rate, to the 2/3 power, and wall heat flux distributions are roughly correlated in terms of distance divided by flame height.

17. Key Words Flame spread, heat flux, wall fires.	18. Distribution Statement This document is available to the U.S. public through the National Technical Information Service, Springfield, Virginia 22161

19. Security Classif. (of this report) Unclassified	20. Security Classif. (of this page) Unclassified	21. No. of Pages	22. Price

Form DOT F 1700.7 (8-72) Reproduction of completed page authorized

PREFACE

The authors wish to acknowledge Mr. W. Rinkinen and Mr. D. Wagger for their support in conducting the heat transfer experiments. Special recognition is given to Prof. A. Kulkarni of the Pennsylvania State University who served as a summer faculty participant in the initial experimental phase of this work. Also we wish to thank Dr. T. Eklund of the Federal Aviation Administration Technical Center for his continued support as technical monitor for this study.

TABLE OF CONTENTS

	Page
INTRODUCTION	1
Purpose	1
Background	1
Objective	4
DISCUSSION	4
Experiments	4
Theoretical Aspects	6
Flame Length	11
Wall Heat Flux	12
Flame Spread	13
Results and Analysis	16
Flame Height	17
Wall Heat Flux	19
Flame Spread Characteristics	20
CONCLUSIONS	24
BIBLIOGRAPHY	24
APPENDIX A.	27
APPENDIX B.	29

LIST OF FIGURES

		Page
Figure 1.	Schematic of apparatus	30
Figure 2.	Photograph of apparatus	31
Figure 3.	Wall heat flux for particle board irradiated at 2.5 W/cm^2	32
Figure 4.	Flame height (to tips) for particle board irradiated at 2.5 W/cm^2	33
Figure 5.	Combustion boundary layer problem	34
Figure 6.	Flame spread problem	34
Figure 7.	Peak energy release rates	35
Figure 8.	Flame height correlation	36
Figure 9.	Wall heat flux distribution (6 pages)	37 - 42
Figure 10.	Wall heat flux for steady wall fires correlated with flame height. •CH_4 line burner flame [15], □ Liquid saturated wall flame [16]	43
Figure 11.	Wall heat flux correlated using flame height	44
Figure 12.	Wall heat flux correlated using flame height and energy release rate	45
Figure 13.	Theoretical wall heat flux results for $\chi_r = 0.2$	46

LIST OF TABLES

		Page
Table 1.	Flame Heat Transfer Characteristics - 80% Average Peak	18
Table 2.	Material Flame Spread Properties	22
Table 3.	Propensity for Flame Spread	23

NOMENCLATURE

a	parameter, Eq. (18)
b	parameter, Eq. (19)
c, c_p	specific heat
C_e	entrainment coefficient
C_f	friction coefficient
E	energy release by chemical reaction
g	gravitational acceleration
k	thermal conductivity (used in flame spread analysis)
L	effective heat of gasification, Eq. (40)
m	mass of fuel gasified
Pr	Prandtl number
q	heat transfer
r	effective stoichiometric oxygen/fuel mass ratio
St	Stanton number
t	time
T	temperature
u,v	gas phase velocity components
V	spread velocity
x,y	coordinates
Y	mass fraction
z	normalized y coordinate, Eq. (9)
β	heat transfer parameter, Eq. (36)
δ	characteristic length
ΔH	heat of reaction per mass of fuel
ΔH_{ox}	heat of reaction per mass of oxygen
ε	mixing factor

η	dimensionless variable, (z/δ)
λ	thermal conductivity (in heat transfer analysis)
ρ	density
τ	shear stress
χ_r	radiative fraction of E
θ	$T - T_\infty$
Φ	flame heating parameter, Eq. (39)

Subscripts

b	burnout
c	convective
e	external
f	flame
g	gas
ig	ignition
m	maximum
ox	oxygen
p	pyrolysis
r	radiative
s	surface
w	wall
∞	ambient

Superscripts

$(\dot{\ })$	per unit time
$()'$	per unit length
$()''$	per unit area
$()'''$	per unit volume

EXECUTIVE SUMMARY

This study has explored a strategy for predicting upward flame spread. It has been done in the context of a larger effort aimed at characterizing the performance of aircraft lining materials in fire and, therefore improving the fire safety of aircraft cabin furnishings.

Six materials have been extensively studied and their flame spread properties are summarized from previous work and the present study. These properties bear on the material's ignitability and its flame spread, both downward and upward, on a vertical surface.

The primary results of the present study show that the flame height for wall fires appears to depend only on the energy release rate of the fuel burning. Moreover, the total heat transfer rate from a wall flame to its adjacent non-pyrolyzing surface region appears to depend only on position from the pyrolyzing region and its energy release rate. It can be shown that the magnitude of this flame heat flux and its extent over the non-pyrolyzing surface region controls the rate of upward flame spread. It was further shown that the burning time or alternatively, the amount of energy release in burning also bears on the rate and propensity of spread.

INTRODUCTION

PURPOSE.

The general purpose of this study is to develop a predictive methodology for surface flame spread in terms of measurable material parameters and engineering formulae. The intent is to examine the feasibility of supplanting relative material flammability rankings with a more scientific framework for use in the evaluation of fire hazards. This work supports the aircraft cabin safety fire program of the FAA Technical Center by providing support for its development of improved test procedures for aircraft interior finishes and furnishings.

BACKGROUND.

This report deals with a phase of the problem; namely, the heat transfer of wall flames and its relationship among different materials. Specifically vertical sections of materials of fixed size, nominally 28 x 28 cm, were irradiated by infra-red heaters and burned. In a related study by Walton and Twilley (1984), energy and mass release rates were measured. Here, the flame height and total heat flux to a cooled wall above the sample were measured. Six materials, representative of aircraft and building interior applications were studied. Complementary data on their radiative ignition and opposed flow flame spread characteristics have been previously reported by Harkleroad, et al. (1983). Results of these previous studies will be summarized herein as they relate to the general purpose of this effort.

The flammability of materials is usually assessed by means of its relative performance in a standard test. Various test methods dominate practice in different countries, but no common denominator or conversion factor exists to relate their results. Indeed, the rationales for their conception, or their intended application, probably differ from test to test. Consequently, success at correlating their results with actual fire behavior must be viewed with scrutiny. Some examples of the results of such exercises have been

reported (Quintiere, 1982; Parker, 1982; Quintiere, 1985). In those analyses some factors, such as energy release, material thermal properties, and ignition temperature, have been discussed in terms of their relationship to fire growth and possible correlation relationships. It should be apparent, however, that different fire scenarios will warrant different factors. Hence, only through analysis and the means of acquiring appropriate data will successful correlations be likely.

One approach, which circumvents analysis, is physical scale modeling. For fire problems similitude modeling is incomplete. Nevertheless, "pressure" modeling does offer a viable alternative, and Alpert (1983) has recently demonstrated its characteristics for wall fires. In that study, materials were burned in various small-scale configurations at environmental pressure levels above a normal atmosphere.

Of course, both scaling and analytic approaches to wall fires must match full-scale performance in various settings. Full-scale "data-bases" include post-crash fire growth within aircraft cabins by Sarkos et al. (1982), studies in support of a standard room fire test in the United States by Lee (1984), and similar work on a French corner test for wall-linings by Hognon (1983). Although some attempts at predicting fire growth on room surface linings have been put-forth by Smith (1981) and Steckler (1983), these are either incomplete or contain empirical aspects. In order to develop the basis for such room fire growth models further, a more systemmatic approach is being pursued.

One aspect of fire growth on a wall surface is the flame spread component itself. Needless to say that the burning rate, its behavior over time and its response to the room environment, is not unimportant. For the flame spread component, the simplest analytical description is adopted to, at least, organize the attack on this problem. In that sense, spread is subdivided into concurrent flow spread (in the direction of the local gas flow) and opposed flow spread (opposite to the local gas flow). Also, both cases are treated as applicable to a thermally thick solid, which can be shown justifiable for most common materials of thicknesses greater than 1 mm. For opposed flow spread deRis (1969) obtains

$$V = \frac{(k\rho c)_g V_g (T_f - T_{ig})^2}{(k\rho c)(T_{ig} - T_s)^2} \tag{1}$$

in which $k\rho c$ are the solid's thermal properties, $(k\rho c)_g$ are the corresponding gas properties, V_g is the opposed flow speed, T_f the adiabatic flame temperature, T_{ig} the ignition or pyrolysis temperature, and T_s the upstream solid surface temperature. The corresponding concurrent flow case, given by Sibulkin and Kim (1977), is

$$V = \frac{(\dot{q}_f'')^2 \, \delta_f}{k\rho c (T_{ig} - T_s)^2} \tag{2}$$

where $\dot{q}_f''$ is the maximum heat flux at the pyrolysis front, and δ_f is an effective flame heat transfer distance measured from the end of the pyrolysis region. If we consider $\dot{q}_f''$ to be uniform over a flame extension region δ_f and zero beyond, then we should modify Eq. (2) by multiplying $k\rho c$ by $\pi/4$. In previous studies by Harkleroad et al. (1983) and Quintiere et al. (1983) it was shown how $k\rho c$, T_{ig} and the numerator of Eq. (1) could be estimated from an experimental technique. Recently, such values have been tabulated for a wide range of materials (Quintiere and Harkleroad, 1984). Consequently, knowledge of $\dot{q}_f''$ and δ_f in Eq. (2) would then complete the required information for wall flame spread.

Thus, an experimental apparatus was designed and constructed to measure the heat flux and flame height above a burning wall section. Provision was made to include external irradiation since most materials do not support sustained combustion on their own. Also provisions were made to substitute a horizontal porous gas burner for the burning vertical slab. This substitution would provide steady-state data in contrast to the unsteady burning of the materials. Hence the gas burner data will complement the material data. Indeed, it helped to guide the analysis and those gas burner results were more extensively discussed by Hasemi (1984). The only other available data on

heat transfer to the wall region above the pyrolysis zone were taken by Ahmad and Faeth (1979) for steady liquid-saturated wick fires.

OBJECTIVE.

The objectives of this study were to measure the heat flux and flame height from wall flames as a result of irradiated burning solid materials and a steady burning distributed line-source gaseous fuel (natural gas). By analysis these data were interpreted and generalized as possible. The bearing of these results on upward flame spread were also to be examined.

DISCUSSION

EXPERIMENTS.

The experimental apparatus of Ahmad and Faeth (1979) was used as a guide in this work, but a radiant source was added. A schematic of the apparatus developed is shown in figure 1, and a photograph of it is shown in figure 2. The sample section was nominally 28 x 28 cm and exposed to radiation from two larger gas-fired porous ceramic heaters. The heaters operated at glowing temperatures which could be varied by changing the air and natural gas supply rates. They were located at each side so that the sample could be viewed normal to its surface. This location and their operating characterisitcs permitted an irradiance level at the sample surface of nominally 1 to 4 W/cm^2. A "Gardon" foil-type heat flux transducer was used to measure the incident flux at the center of an inert sample board. Uniformity over the sample area was within ten percent, and the weighted-average irradiance was 94 percent of the center value.

Above the sample was a flush-mounted contiguous water-cooled copper plate with provision for monitoring incident heat flux at the locations shown in figure 1. Two types of sensors were used - a total heat flux Gardon-type sensor, and an ellipsoidal-type radiometer similar to that described by

Chedraille and Brand (1972). Because of calibration uncertainties in this application, the radiometer data will not be presented here. Also an analysis (appendix A) of the Gardon gage response to convective heat transfer, for a uniform convective heat transfer coefficient (h) over the foil disc, yielded a slight effect of h on the calibration for the sensor used. Moreover, the copper plate was maintained at a nominal temperature of 60°C along with the sensors to prevent condensates from depositing. Cooled side-plates were also included to form a channel and restrict side flow into the flames and preserve two-dimensionality of the boundary layer flow over the plate.

The material to be measured was mounted in an iron-frame holder which could very quickly be inserted in position after the inert sample board was removed. A horizontal copper tube with a line of holes formed a diffusion burner at the base of the sample. This exposed the sample to an ignition-pilot flame of approximately 1 cm height with a rapidly decreasing heat flux with distance from a maximum of roughly 2 W/cm^2 at the lower edge of the sample. Thus, this pilot flame heated the lower edge of the sample in addition to the applied external radiant heat flux. Nevertheless the radiant flux was prevalent over most of the sample surface and was the dominant factor in controlling the burning rate. The ignition behavior was controlled by both the applied radiative heat flux and the pilot flame heat flux.

The procedure for conducting the experiment was to set the irradiance level, wait until it stabilized, and then insert the sample. A video record was made along with automatic data recording and storage on a computer disc. Signals from the heat flux sensors and thermocouples were scanned and averaged over 10- to 15-second intervals, and their averages stored at these time intervals. The experiment was continued until flaming combustion ceased. The flame height records were deduced by observation of the video recordings and a "flame tip" height was based on the distance to the uppermost position of the luminous flames. A height over which continuous flaming occurred was also recorded, but this was more difficult to observe with consistency and did not always occur above the sample's pyrolysis region. In other words, continous flaming did not always occur over the entire sample face as exposed to the uniform radiation. A typical result showing the measured incident total heat

flux at the six positions and the corresponding flame tip height as a function of time is shown in figures 3 and 4, respectively. The time in figure 3 is measured from t=0 at the instant of sample insertion, but in figure 4, t=0 corresponds to the instant of sample ignition. It should be noted that the unshielded radiant flux from the heaters was subtracted from the flux measurements so as to yield just the flame heat flux. This superposition view point was justified by the expectation that the flame is likely to be optically thin, and by measurements with a natural gas flame simulating the sample flame. The natural gas diffusion flame was initiated by a horizontal porous burner at the base of the heat transfer plate.

THEORETICAL ASPECTS.

Before proceeding to analyze and report the results, it was felt necessary to establish a theoretical basis for analysis. The most relevant previous study was by Ahmad and Faeth (1979) who correlated their heat flux data using a turbulent-flame-sheet model based on convective heating alone. Moreover their measured heat flux values above the pyrolysis zone for alcohol-saturated wall fires show a convective component of nearly 80 to 90 percent. Also the heat flux in the flame region was nearly constant, then sharply dropped off as aproximately $x^{-7/3}$. In contrast, the work by Orloff et al. (1975) for flame spread on polymethyl-methacrylate show a radiative component of 50 to 75 percent. Thus, the composition of this heat flux is expected to be at least material and scale dependent.

Another useful background result is that the flame height appears to be solely dependent on energy release rate for wall fires. This was proposed by Delichatsios (1984) and indeed was demonstrated recently by Hasemi (1984). As a first step, a simple model will be put forth to provide a framework for approaching an analysis of the data and for identifying points for further study. The model will only deal with the effects in the reacting zone, and the chemical effects will be treated only as a source of energy in the energy equation. Thus diffusion of species will not be explicitly included nor will pyrolysis effects of the solid. The fuel might be considered to originate at a line-source so that we attempt to simulate flame heating of the downstream

non-pyrolyzing region. In fact, the surface temperature of the solid will be treated as uniform and at the ambient temperature T_∞, since the surface temperature will be much less than the flame temperatures. A schematic of the posed problem is shown in figure 5. The two-dimensional governing equations follow:

$$\frac{\partial(\rho u)}{\partial x} + \frac{\partial(\rho v)}{\partial y} = 0 \tag{3}$$

$$\rho\left(u \frac{\partial u}{\partial x} + v \frac{\partial u}{\partial y}\right) = g\left(\rho_\infty - \rho\right) + \frac{\partial}{\partial y}\left(\mu \frac{\partial u}{\partial y}\right) \tag{4}$$

$$\rho c_p\left(u \frac{\partial \Theta}{\partial x} + v \frac{\partial \Theta}{\partial y}\right) = \frac{\partial}{\partial y}\left(\lambda \frac{\partial \Theta}{\partial y}\right) + \frac{\partial \dot{q}''_r}{\partial y} + \dot{q}''' \tag{5}$$

where $\Theta = T - T_\infty$, $\dot{q}''_r$ is the radiative flux, and $\dot{q}'''$ is the energy release due to chemical reaction. The boundary conditions are:

$$\begin{aligned} &y = 0, \ \Theta = u = v = 0 \\ &y \to \infty, \ \Theta = u = 0 \end{aligned} \tag{6}$$

These equations are integrated over $0 \leq y < \infty$ to yield, from Eq. (4):

$$\frac{d}{dx}\int_0^\infty \rho u^2 dy = \int_0^\infty g\left(\rho_\infty - \rho\right) dy - \tau_w \tag{7}$$

where $\tau_w = \mu\left(\frac{du}{dy}\right)_{y=0}$, the wall shear stress.
Similarly, integration of Eq. (5) gives

$$c_p \frac{d}{dx}\int_0^\infty (\rho u \Theta) dy = - \dot{q}''_{w,c} - \dot{q}''_r + \int_0^\infty \dot{q}''' dy \tag{8}$$

where $\dot{q}''_{w,c} = \left(\lambda \frac{\partial\Theta}{dy}\right)_{y=0}$, the convective heat flux to the wall, and $\dot{q}''_r$ is the flame radiative heat loss. It is further assumed that the flame is optically thin which implies that $\dot{q}''_r$ can be assumed equally split between the wall and the environment. The mass and enthalpy aditions of the fuel have been neglected since we expect these source terms to be small compared with the total mass and energy transfers over the flame region, i.e. $\dot{m}'$ is small compared to $(\rho v)_{y\to\infty}$, the air entrained. Furthermore, the energy release rate will be based on the oxygen consumption rate, i.e.,

$$\int_0^\infty \dot{q}'''dy = -\frac{(\rho v)_{y\to\infty} \cdot Y_{ox,\infty}}{\varepsilon r} \Delta H = -(\rho v)_{y\to\infty} \frac{Y_{ox,\infty}\Delta H_{ox}}{\varepsilon} \tag{9}$$

where ΔH_{ox} is the heat of reaction per unit mass of oxygen consumed (approximately 13 kJ/g for most hydrocarbons), and ε is a mixing factor implying that some oxygen is not immediately reacted.

In addition, the flame radiation will be assumed as a constant fraction χ_r of the energy release,

$$\dot{q}''_r = \chi_r \int_0^a \dot{q}'''dy \tag{10}$$

Tamanini (1979) demonstrated that this assumption is not as good as using a "soot-band" model, but his results suggest that it is not an unreasonable approximation. The wall component is then

$$\dot{q}''_{w,r} = \dot{q}''_r/2 \tag{11}$$

for the optically thin case. A more suitable expression based on the radiation transfer equation is given in appendix B, but will not be pursued here.

In order to eliminate the density dependence, the following transformation is made,

$$z = \int (\rho/\rho_\infty)dy \tag{12}$$

The integral equations then become

$$\rho_\infty \frac{d}{dx} \int_0^\infty u dz + (\rho v)_{y\to\infty} = 0 \tag{13}$$

$$\rho_\infty \frac{d}{dx} \int_0^\infty u^2 dz = \int_0^\infty \rho_\infty g \frac{\Theta}{T_\infty} dz - \tau_w \tag{14}$$

$$\rho_\infty c_p \frac{d}{dx} \int_0^\infty u\Theta dz = \rho_\infty Y_{ox,\infty} \frac{\Delta H_{ox}}{\varepsilon} (1 - \chi_r) \frac{d}{dx} \int_0^\infty u dz - \dot{q}''_{w,c} \tag{15}$$

where $\mu/\rho = \mu_\infty/\rho_\infty$, $k/\rho c_p = k_\infty/\rho_\infty c_p$, and c_p are all assumed constant.

The equations can be integrated and solved by introducing the profiles,

$$u = u_1(x)F(\eta) \tag{16a}$$

$$\Theta = \Theta_1(x)G(\eta) \tag{16b}$$

where $\eta = z/\delta(x)$ and δ is the boundary layer thickness. Also u and Θ are taken to be zero for $\eta > 1$.

Following Liburdy and Faeth (1978) for the high Reynolds number regime of a turbulent wall plume,

$$(\rho v)_{y\to\infty} = - \rho_\infty C_e u_m \tag{17}$$

$$\tau_w = C_f \left(\rho_\infty u_m^2/2\right) \tag{18}$$

FAA WJH Technical Center
00092809

$$\dot{q}''_{w,c} = St\ (\rho_\infty c_p u_m \theta_m) \tag{19}$$

with the local maximum, $u_m = au_1$ and $\theta_m = b\theta_1$; and where C_e the entrainment constant, C_f the friction coefficient, and St the Stanton number are all constant. Also by the Coburn analogy,

$$St = Pr^{-2/3} C_f/2 \tag{20}$$

Under these assumptions, it can be shown that

$$\left.\begin{aligned} u_1 &= u_o x^{1/2} \\ \theta_1 &= \theta_o \\ \text{and} \quad \delta &= \delta_o x \end{aligned}\right\} \tag{21}$$

can satisfy Eqns. (13-15). Upon substitution Eq. (13) yields:

$$\delta_o = \frac{2}{3}\, aC_e / \int_0^1 F d\eta; \tag{22}$$

Eq. (14) yields:

$$u_o^2\ \delta_o 2 \int_0^1 F^2 d\eta = \frac{g\delta_o\theta_o}{T_\infty} \int_0^1 G d\eta - \frac{C_f a^2 u_o^2}{2}\ ; \tag{23}$$

and Eq. (15) yields:

$$c_p \theta_o \delta_o\ \frac{3}{2} \int_0^1 FGdy = \frac{Y_{ox,\infty} \Delta H_{ox} (1-\chi_r)\delta_o}{\epsilon}\ \frac{3}{2} \int_0^1 F d\eta - \frac{c_p abC_f Pr^{-2/3}\theta_o}{2} \tag{24}$$

Reasonable profiles, to satisfy the boundary conditions and the physical behavior suggested by analogous problems, were taken as

$$F(\eta) = \eta^{1/7} (1 - \eta) \tag{25}$$

and $$G(\eta) = \eta (1 - \eta)^2 \tag{26}$$

for which at $\eta = 0$, $u = \Theta = 0$ and at $\eta = 1$, $u = \Theta = \frac{\partial\Theta}{\partial\eta} = 0$ as well as the (1/7)th power holds for u near the wall. It follows that $a = 7/8^{8/7} = 0.650$ and $b = 4/27 = 0.148$. Consequently, the solutions for δ_o, u_o, and Θ_o are

$$\delta_o = 1.06\ C_e, \tag{27}$$

$$\Theta_o = \frac{1.99\ a\Theta_f C_e}{0.408\ aC_e + abC_f/Pr^{2/3}} \tag{28}$$

where $\Theta_f \equiv Y_{ox,\infty} \frac{\Delta H_{ox}}{\varepsilon} (1 - \chi_r)/c_p$; and

$$u_o = 0.52\ aC_e \left\{ \frac{g\Theta_f}{T_\infty(0.675\ aC_e + a^2C_f/2)(0.408\ aC_e + abC_f/Pr^{2/3}} \right\}^{1/2} \tag{29}$$

Liburdy and Faeth (1978) give results that suggest $C_e = 0.096$ for $C_f = 0.015$ and $Pr = 0.7$. Thus a solution is found.

FLAME LENGTH. An expression for flame length can be derived by assuming that the reaction zone ends when the fuel is completely consumed. That is, the entrainment rate of oxygen primarily controls the flame length. This can be expressed as

$$\int_o^{x_f} Y_{ox,\infty} (-\rho v)_{y\to\infty} dx = \varepsilon r \dot{m}' \tag{30}$$

where x_f is the flame length, r is the stoichiometric oxygen to fuel mass ratio, $\dot{m}$ is the fuel supply rate and ε is a mixing factor which depends on the fluid dynamics of the flame. From Eq. (30) together with Eqns. (17), (21) and (27) and also by realizing that

$$r\dot{m}' = \dot{E}'/\Delta H_{ox} \tag{31}$$

where $\dot{E}'$ is the energy release rate per unit width, it follows that

$$x_f = \left(\frac{1.5\ \varepsilon\dot{E}'}{\rho_\infty Y_{ox,\infty}\Delta H_{ox} a C_e u_o}\right)^{2/3}. \tag{32}$$

Delichatsios (1984) finds, for turbulent wall flames,

$$x_f = 4.65\left(\frac{\dot{E}'}{c_p T_\infty \rho_\infty \sqrt{g}}\right)^{2/3} \tag{33}$$

which is functionally similar to Eq. (32) by substitution of Eq. (29) for u_o. Hasemi (1984) finds the coefficient for Eq. (33) is 6.1 for methane line-burner flames against a wall when x_f pertains to the height of the upper most flame tips. He obtains 2.9 as the coefficient for the height of the continuous flame region.

WALL HEAT FLUX. An expression for wall heat transfer over the flaming zone can also be derived. From Eq. (9), (10), (11), (21) and (25)

$$\dot{q}''_{w,r} = \frac{0.306\ \rho_\infty Y_{ox,\infty}\Delta H_{ox}\chi_r u_o \delta_o x^{1/2}}{\varepsilon}, \tag{34a}$$

and from Eq. (19), (20), (21)

$$\dot{q}''_{w,c} = \frac{C_f}{2Pr^{2/3}}\rho_\infty c_p u_m \theta_m = \frac{C_f}{2Pr^{2/3}}\rho_\infty c_p ab\theta_o u_o x^{1/2} \tag{34b}$$

The total wall flux is

$$\dot{q}_w'' = \rho_\infty u_o \left(\frac{abC_f c_p \theta_o}{2Pr^{2/3}} + \frac{0.306\ \chi_r Y_{ox,\infty} \Delta H_{ox} \delta_o}{\varepsilon} \right) x^{1/2} \tag{35}$$

It will be of interest to introduce dimensionless terms and x_f seems to be an appropriate normalizing factor for x. Therefore,

$$\dot{q}_w'' = \beta (x/x_f)^{1/2} \tag{36a}$$

where

$$\beta = \rho_\infty u_o \left(\frac{abC_f c_p \theta_o}{2Pr^{2/3}} + \frac{0.306\ \chi_r Y_{ox,\infty} \Delta H_{ox} \delta_o}{\varepsilon} \right) \left(\frac{1.5\ \varepsilon \dot{E}'}{\rho_\infty Y_{ox,\infty} \Delta H_{ox} a C_e u_o} \right)^{1/3} \tag{36b}$$

Equation (36) suggests that β depends weakly on $\dot{E}'$ and $\dot{q}_w''$ increases with x/x_f to the 1/2 power in the reacting zone. The motivation for expressing the heat flux in this form is to examine the extent of similarity in the flame zone. Indeed, this strategy of plotting $\dot{q}_w''$ as a function of x/x_f was used in examining the data and showed remarkable universality. Although it will be shown that Eq. (36) does not follow the data well, its value is in representing the wall heat flux in terms of measurable quantities; namely, $\dot{E}'$ and χ_r. These dependencies need to be further resolved through experimental correlations and more complete theoretical analyses incorporating better models for radiation and wall turbulence. It should be noted that the theoretical results for $\dot{q}_w''$ by Ahmad and Faeth (1979) give a dependence of $x^{0.2}$ in the wall pyrolysis region and slightly concave downward in the combusting region downstream. Moreover analogous turbulent natural convection results might suggest that the heat flux be constant and independent of x.

FLAME SPREAD. Although flame spread rate was not explicitly addressed in the experiments, some estimates of flame spread rates could be made with the data. A starting point for this analysis would be Eq. (2); however, the burn-

out of the material must also be addressed. Coordinates are shown in figure 6 which depict the location of the burn-out front x_b, the pyrolysis front x_p, and the flame tip position x_f -- all measured from the leading edge of the solid. Expressions for x_p and x_b can be derived from kinematic arguments by assuming that the front velocity is slowly varying in time. For example, the pyrolysis front velocity can be approximated as

$$V_p = \frac{dx_p}{dt} \cong \frac{x_p(t + t_f) - x_p(t)}{t_f} = \frac{x_f(t) - x_p(t)}{t_f} \tag{37a}$$

where t_f is the time for the pyrolysis front to move across the flame heat transfer region, $x_f(t) - x_p(t)$. Thus, $x_p(t + t_f)$ will coincide with $x_f(t)$ when the initial surface temperature T_s has been raised to T_{ig} by a constant flame heat flux to the wall $\dot{q}''_w$. From one-dimensional heat conduction theory, it follows that under these conditions for a semi-infinite solid

$$t_f \cong k\rho c \left[(T_{ig} - T_s)/\dot{q}''_w\right]^2 . \tag{37b}$$

Hence Eq. (37) is identical to the more rigorously derived expression given by Eq. (2).

In a parallel manner, an expression for the burn-out front velocity can be derived. By a difference approximation

$$V_b = \frac{dx_b}{dt} \cong \frac{x_b(t + t_b) - x_b(t)}{t_b} = \frac{x_p(t) - x_b(t)}{t_b} \tag{38a}$$

where t_b is the duration of burning at a given position x. If t_b is independent of x or slowly varying with x, then by definition, since burning commences at $x_p(t)$ at time t, it follows that $x_b(t + t_b)$ coincides with $x = x_p(t)$ at time $t + t_b$. Also if m represents the volatizable mass, then the burn-out time is defined by

$$\int_0^{t_b} \dot{m}''(x)dt = m''. \tag{38b}$$

In general both t_f and t_b can depend on x, but will be considered as constants in the subsequent illustrative analysis. Appropriate initial conditions are also necessary and can be considered as follows. In any real problem of upward spread, an ignition process will precede flame spread. The ignition source may be a radiative source, a flame source, and transient or constant in application. In any case, at time t=0 (ignition), some finite region x_{p_o} of material will be undergoing pyrolysis. Let us assume that the ignition source is removed at t=0 also. Furthermore let us consider a linearized version of Eq. (32) to permit ease in illustrating some solution characteristics, i.e.

$$x_f = k_f\dot{E}''x_p \text{ for } t < t_b \text{ and } x_f - x_b = k_f\dot{E}''(x_p - x_b) \text{ for } t > t_b.$$

It can be shown from Eq. (37a) that for $o < t < t_b$,

$$x_p = x_{p_o} e^{(k_f\dot{E}'' - 1)\, t/t_f} \tag{39a}$$

and for $t > t_b$ using Eqns. (37a and 38a) with

$x_p = x_{p_1}$ and $x_b = x_{p_o}$ at $t = t_b$,

$$x_p - x_b = (x_{p_1} - x_{p_o})e^{[k_f\dot{E}'' - (t_f/t_b) - 1](t - t_b)/t_f} \tag{39b}$$

where $\dot{E}''$ has been assumed constant over the burn time t_b. These results should be viewed as qualitative, but they show the importance of $\dot{E}''$ and t_f/t_b in spread. Indeed a recent more rigorous analysis by Saito et al. (1984) also

show the prominence of these terms. Moreover Eq. (39b) shows that the spread rate will only be acceleratory provided $k_f \dot{E}'' - t_f/t_b > 1$. Thus a criterion for self-propagation or the conditions necessary for such is revealed.

RESULTS AND ANALYSIS.

The transient aspect of burning materials is difficult to analyze because their degradation behavior is not generally understood. For example, charring, melting, shrinking and significant regressing were all observed among the samples tested. Transient effects in the gas-phase are very fast, so that a quasi-steady analysis is justifiable for gas-phase phenomena. Consequently, the data will be analyzed over the peak burning conditions of the sample and the corresponding flame heights and heat fluxes will be reported. The transient behavior of the solid will be characterized by a burning time which will also be reported.

Peak burning conditions were somewhat arbitrarily defined as follows:

(1) the maximum value recorded by the first heat flux sensor (at x_1) was located, and the times at which 80 percent of this maximum first occurred on either side of the peak were located;

(2) average values for each heat flux sensor were determined for these times, i.e.,

$$\bar{\dot{q}}_i'' = \frac{1}{(t_2 - t_1)} \int_{t_1}^{t_2} \dot{q}_i''\, dt; \qquad (40)$$

(3) this procedure was also applied to the corresponding flame height measurements;

(4) a similar procedure was applied to the energy release rate data of Walton and Twilley (1984) for the same materials, but evaluated at somewhat higher external radiative heating conditions.

The burning time (t_b) was defined by locating the times bounding the peak heat flux for the sensor at x_1 at which the flux was 10 percent of its maximum. These "80% peak-average" values and the burn times are tabulated in table 1 for the heat transfer experiments. The energy release rates were interpolated from the peak values plotted in figure 7 as derived from Ref. [1].

FLAME HEIGHT. Figure 8 displays the height of the visible flame tips with the energy release rate per wall fire width, $\dot{E}' = \dot{E}'' x_p$. Although the data trend follows the correlations of Hasemi (1984) and Delichatsios (1984), there is considerable scatter. For the most part, the scatter is believed due to the inconsistency in deriving flame height and energy release from two independent devices. It does not necessarily mean that these devices are incompatible, except where a horizontal burn configuration was used in the calorimeter for the flexible foam material. The scatter does suggest that greater care in data accuracy and interpretation is needed when x_f is nearly equal to x_p in magnitude, when the burning time is short, and when the composite nature of the sample produces multiple effects during combustion. All of these factors probably contributed to the carpet, aircraft panel and rigid foam samples. Also a visible observation of transient flaming is probably not ideal for a flame height measurement although consistency among several observers was noted.

It is interesting, and essential for the development of numerical results, to determine ε, the ratio of oxygen present to stoichiometric oxygen needed for complete combustion. This is a mixing factor that represents the inability for the entrained oxygen to react instantly with the fuel available. From Eq. (32) and the coefficient given by Hasemi for the flame tips in Eq. (33), ε is computed as 6.6 for $Y_{ox,\infty} = 0.233$, i.e., air. Tamanini (1977) computes a corresponding value of 9 for a turbulent axisymmetric flame plume, but such values (e.g., 5 to 20) are abundant in the literature. Nevertheless, the parameter ε is a valuable fluid dynamic modeling parameter. If the coefficient for the continuous flame height is used instead, i.e., 2.9 in Eq. (33), then ε becomes 3.13. Thus, about 3 times the stoichiometric air is entrained over the continuous combusting region, and 6.6 times stoichiometric air is entrained over the entire combusting zone to the flame tip.

TABLE 1. FLAME HEAT TRANSFER CHARACTERISTICS - 80% AVERAGE PEAK

Material	$\dot{q}''_e$ (W/cm^2)	$\dot{q}''_1$ (W/cm^2)	$\dot{q}''_2$ (W/cm^2)	$\dot{q}''_3$ (W/cm^2)	$\dot{q}''_4$ (W/cm^2)	$\dot{q}''_5$ (W/cm^2)	$\dot{q}''_6$ (W/cm^2)	t_b (s)	$\dot{E}''$ (kW/m^2)	x_f (cm)
Douglas Fir Particle Board	1.7[1]	1.71	0.72	0.29	0.15	0.08	0.06	432.	140.	66.
	1.7	1.72	0.73	0.30	0.15	0.09	0.07	209.	140.	73.
	2.5	1.88	0.76	0.30	0.17	0.12	0.11	209.	165.	61.
	3.5	1.79	0.94	0.35	0.16	0.10	0.08	404.	195.	90.
Flexible Foam	1.8	2.62	1.84	1.01	0.51	0.31	0.22	72.	525.	116.
	2.5	2.35	1.46	0.70	0.30	0.19	0.13	57.	570.	96.
	3.5[2]	1.99	0.98	0.43	0.22	0.14	0.11	45.	645.	110.
	3.5[2]	2.3	1.18	0.50	0.28	0.18	0.14	47.	645.	112.
Carpet (nylon/wool blend)	2.5	1.98	1.20	0.70	0.34	0.20	0.13	130.	75.	88.
	3.0	2.63	1.69	0.75	0.36	0.20	0.14	101.	160.	105.
	3.0[3]	1.89	0.84	0.27	0.14	0.08	0.08	-	180.	67.
	3.6	2.65	1.46	0.65	0.33	0.19	0.15	104.	220.	39.
Foam, Rigid	1.9	0.51	0.08	0.04	0.02	0.01	0.01	28.	110.	39.
	2.4	1.05	0.20	0.08	0.05	0.03	0.02	110.	130.	39.
	3.0	1.12	0.20	0.08	0.05	0.04	0.03	137.	150.	43.
	3.0[1]	1.15	0.22	0.10	0.05	0.04	0.03	143.	150.	42.
PMMA	1.5	2.16	2.13	1.59	0.93	0.46	0.30	1664.	400.	125.
	1.7	2.40	2.27	1.71	0.99	0.51	0.32	1558.	505.	138.
	2.4	1.96	2.51	2.14	1.42	0.82	0.51	1331.	590.	156.
	3.0	2.14	2.64	1.96	1.47	0.91	0.63	1112.	705.	167.
Aircraft Panel, epoxy fiberite	2.5	0.80	0.30	0.12	0.07	0.04	0.03	43.	40.	68.
	3.0	1.12	0.29	0.10	0.05	0.04	0.03	29.	55.	48.
	3.7	1.06	0.33	0.13	0.07	0.05	0.04	28.	80.	61.

[1] Specimen burns, extinguishes, reignites - results from first burn period
[2] Energy release rate from horizontal burn configuration
[3] Sample fell from holder after peak burn

WALL HEAT FLUX. The wall total heat flux distributions are presented in figures 9A through F for each of the materials. The distance x is measured from the base of the sample as indicated in figure 1. The effect of the external irradiance level is not marked, probably because the change in energy release rate inferred from figure 7 is not large enough. Also transient and particular material characteristics must have some bearing here. For the most part the materials display a decreasing flux with distance, $\dot{q}''_w \propto x^{-p}$ where p is about 2.4. This is consistent with the distributions measured by Ahmad and Faeth (1979) outside of the flame zone, and can be approximately described by the model offered by Liburdy and Faeth (1978). In the case of PMMA, the flux displays a maximum or nearly constant value of 2 to 3 W/cm^2 in the flame zone. This is indicative of the combustion zone results found by Ahmad and Faeth (1979). Indeed, the level of heat flux in this combusting region is similar despite the different fuels.

As a result of this observation it was thought appropriate to scale the distance x with the flame length x_f in considering the flux distribution. Such an analysis was performed by Hasemi (1984) for CH_4 line burner fires against a wall with $\dot{E}'$ ranging from about 10 to 100 kW/m. Also he reprocessed the data of Ahmad and Faeth (1979) into this form; and those results, along with a sample of Hasemi's data in the apparatus of figures 1 and 2, are shown in figure 10. No definitive understanding of the effects of fuel type, fuel configuration and energy release have been extracted from these results at this time. The universality of the correlation with the displayed scatter is intriguing and bears further study.

As a consequence of the burner analysis the data of figure 9 were plotted in terms of x/x_f with the result shown in figure 11. This approach does significantly collapse the data and the results are consistent with the correlation in figure 10. The maximum values of recorded heat flux for each material range from about 1 to slightly less than 3 W/cm^2. Thus a universal maximum value does not seem apparent as the data correlation might imply. Either more data need to be derived within the flame region for the materials yielding low maximum fluxes, or the flux distribution depends on energy release rate. The

latter factor is suggested by the theoretical analysis as expressed by Eq. (36) in that $\dot{q}''_w \propto (\dot{E}')^{1/3}$. This was explored further by plotting $\dot{q}''_w/(\dot{E}'')^{1/3}$ from table 1 against x/x_f for the materials. The result is shown in figure 12, and seems to offer no improvement over figure 11 although the maximum value of $\dot{q}''_w/(\dot{E}'')^{1/3}$ is nearly identical for four of the materials. Moreover the scatter here is likely due to the same inconsistencies in the flame height correlation of figure 8 in which the extrapolated energy release data may be at fault.

Finally, the theoretical solution for heat flux will be examined. If χ_r, the radiative fraction, is selected as 0.20 and $Y_{ox,\infty} = 0.233$ (air), it can be shown that β of Eq. (36b) is computed as

$$\beta = (9.81 + 17.7)\ (\dot{E}')^{1/3}/\varepsilon\ \left(kW/m^2\right) \tag{41}$$

where 9.81 represents the convective contribution and 17.7 represents the radiative contribution (with $\dot{E}'$ in kW/m). Two values of ε may be considered: $\varepsilon = 3.13$, suggesting the combustion zone is defined by the continuous flame region which corresponds to $x/x_f = 0.48$; or $\varepsilon = 6.6$, suggesting that the combustion extends to the flame tip, $x/x_f = 1$. Over an appropriate range of $\dot{E}'$, computed results from Eq. (36) are given in figure 13. Although the results for $\varepsilon = 3.13$ are comparable to the data of figures 10 and 11, the x and $\dot{E}'$ dependences are not entirely consistent. Undoubtedly this is due to the simplicity of the theory, its lack of fully addressing the radiative computation more thoroughly and its lack of more specific flame radiative properties for these materials. Preliminary assessments of the radiative component of the wall heat flux has suggested its contribution to be 50 percent or greater. The theoretical result gives 64% for $\chi_r = 0.20$. Thus the radiative effects must be better understood.

FLAME SPREAD CHARACTERISTICS.

A first step has been taken to characterize heat transfer from wall flames so that upward flame spread might be predicted. It is obvious that additional study needs to be given to complete this objective, but the current results

offer at least a framework for analysis. Ultimately a prediction of the transient burning rate or energy release rate is also needed, and models have not been developed for this aspect. Nor has it been shown how results from laboratory calorimetry data can be utilized in such analyses. Some additional data can be presented for the materials considered herein which address some aspects of related flame spread phenomena. For example, downward or lateral spread in air on a vertical surface can be expressed from Quintiere and Harkleroad (1984) as follows :

$$V = \frac{\Phi}{(k\rho c)(T_{ig} - T_s)^2}, \qquad T_{s,min} \leq T_s < T_{ig} \tag{42}$$

where Φ represents a flame heat transfer parameter,

$k\rho c$ is the effective thermal inertia of the solid,

T_{ig} is the effective ignition (piloted) temperature,

T_s is the upstream surface temperature,

and $T_{s,min}$ is the minimum surface temperature necessary for flame spread.

Pyrolysis rate might be approximated as

$$\dot{m}'' = \frac{\dot{q}''_{s,net}}{L} \tag{43}$$

where $\dot{q}''_{s,net}$ is the net surface heat flux which is related to $\dot{q}''_w$, but not exactly identical, due to blowing effects and surface reradiation; L is the effective heat of gasification. Finally, the energy release rate is given as

$$\dot{E}'' = \dot{m}''\Delta H$$

with ΔH the heat of reaction.

Values for these parameters are summarized in table 2. Also some attempt at comparison is made there with similar data by Tewarson (1980). An effective stoichiometric oxygen to fuel ratio and Tewarson's surface temperature at steady burning $T_{s,b}$ are also given. The values for the rigid foam material

(GM-21) show the most disparity between the work at this laboratory [1,14] and those by Tewarson (1980). Also ignition results, not shown, reflect similar disagreement. This is a fire retardant foam that has been stored in a material bank (Nadeau, 1980) for several years. Tewarson used the material in the mid-1970's and our use has been in the last several years. Thus some material change might have occurred, since so many of the compared parameters are different. Of course this is speculation, but could prove an issue for interlaboratory comparisons on material performance.

TABLE 2. MATERIAL FLAME SPREAD PROPERTIES

Ref:	T_{ig} +1 (°C)	$k\rho c$ 1 $(kW/m^2K)^2s$	ϕ 1 $(kW)^2/m^3$	$T_{s,min}$ 1 (°C)	ΔH 2 (kJ/g)	L 2 (kJ/g)	r 2 (gO_2/gfuel)	ΔH 3 (kJ/g)	L 3 (kJ/g)	$T_{s,b}$ 3 (°C)
Particle Board	412	0.93	4.27	275	11.6	4.5	0.89	12.4**	1.7**	457.**
Aircraft Panel	505	0.24	0	505	17.6	3.7	1.34	--	--	--
Flexible Foam	390	0.32	11.7	120	18.8	--	1.44	16.*	1.96*	457.*
Carpet	412	0.68	11.1	265	16.8	2.5	1.28	--	--	--
Rigid Foam (GM31)	435	0.03	4.09	215	21.0	7.8	1.6	13.	3.1	517.
PMMA	378	1.02	14.4	$\leq$90	25.6	1.8	1.95	22-25	1.6	387.

*different flexible foam, GM-21
**different wood, oak

+1. Quintiere and Harkleroad (1984)
2. Walton and Twilley (1984)
3. Tewarson (1980)

Although no direct measurements of upward flame spread were made, Eq. (39) suggests some flame spread characteristics. A spread time t_f can be computed based on the maximum wall heat flux recorded for each run. This can be compared to the burn time t_b and its ratio t_f/t_b suggests a propensity to spread. If this ratio is small then continued spread is likely, and conversely. These results are shown in table 3.

TABLE 3. PROPENSITY FOR FLAME SPREAD

Material	$\dot{q}''_e$ (W/cm^2)	$t_f = (k\rho c)[(T_{ig} - T_\infty)/\dot{q}''_{w,max}]^2$ (s)	t_f/t_b (-)
Particle Board Douglas Fir (1.27 cm)	1.7	484.	1.1
	1.7	478.	2.3
	2.5	400.	1.9
	3.4	441.	1.1
Flexible Foam (2.54 cm)	1.8	63.	0.9
	2.5	78.	1.4
	3.5	109.	2.4
	3.5	82.	1.7
Carpet (nylon/wool blend)	2.5	264.	2.0
	3.0	150.	1.5
	3.0	290.	2.9
	3.6	147.	1.4
Rigid Foam, GM-31 (2.54 cm)	1.9	197.	7.03
	2.4	46.	0.4
	3.0	41.	0.3
	3.0	39.	0.3
PMMA, Type G	1.5	277.	0.2
	1.7	224.	0.1
	2.4	205.	0.2
	3.0	185.	0.2
Aircraft Panel (epoxy fiberite)	2.5	874.	20.
	3.0	446.	15.
	3.7	498.	18.

If t_f/t_b is greater than 1 the burning may cease before the pyrolysis front has a chance to traverse the distance $x_f - x_p$, and hence propagation may cease. A more complete understanding of the transient effects together with a more complete solution to Eqns. (37) and (38) is necessary. Temporarily at least some appreciation of the phenomenon can be discerned from t_f/t_b.

CONCLUSIONS

Two key results emerge from this study. First, flame height for wall flames is primarily proportional to the energy release rate to the 2/3-power. Second, wall heat flux seems to have an approximately universal distribution when plotted with distance normalized by flame length (x/x_f). These results have profound potential in simplying predictive methods of flame spread. Therefore, further work should be conducted to more fully establish the limits and general application of these results.

BIBLIOGRAPHY

Ahmad, T. and Faeth, G. M. (1979). Seventeenth Symp. (Int.) on Combustion, The Combustion Institute, pp. 1149-1160.

Alpert, R.L. (1983). "Pressure Modeling of Fire Growth on Char-Forming and Laminated Materials", FMRC J.I. OGO-N3.BU, RC83-BT-11, Factory Mutual Res. Corp.

Chedaille, J. and Brand, Y. (1972). Measurements in Flames, Vol. 1 of Industrial Flames, ed. by J.M. Beer and M.W. Thring, Int. Flame Res. Foundation, Crane, Russak and Co., Inc., NY.

deRis, J.N. (1969). Twelfth symp. (Int.) on Combustion, The Combustion Institute, pp. 241-252.

Delichatsios, M.A. (1984). Modeling of Aircraft & Cabin Fires, NBS-GCR-84-473, Nat. Bur. Stand.

Gardon, R. (1953). The Review of Scientific Instruments, Vol. 24, No. 5.

Harkleroad, M., Quintiere, J. and Walton, W. (1983). "Radiative Ignition and Opposed Flow Flame Spread Measurements on Materials", U.S. Dept. Trans., Fed. Aviation Admin. Tech. Ctr., DOT/FAA/CT-83/28.

Hasemi, Y. (1984). Fire Science and Technology, Vol. 4, No. 2, p. 75.

Hognon, B. (1983). "Behavior in Fire of Interior Wall Coverings and Linings", Centre Scientifique et Technique du Batiment, France.

Lee, B.T. (1984). "Standard Room Fire Test Development at the National Bureau of Standards", Symp. on Application of Fire Science to Fire Engineering, Amer. Soc. Testing and Materials/Soc. Fire Prot. Engrs., Denver.

Liburdy, J.A. and Faeth, G.M. (1978). Journal of Heat Trans., Vol. 100, No. 2, Amer. Soc. Mech. Engrs.

Nadeau, H.G. ed. (1980). "Materials Bank Compendium of Fire Property Data", Products Research Comm.

Orloff, L., deRis, J. and Markstein, G.H. (1975). Fifteenth symp. (Int.) on Combustion, The Combustion Institute, p. 183.

Parker, W.J. (1982). "As Assessment of Correlations Between Laboratory and Full Scale Experiments for the FAA Aircraft Fire Safety Program, Part 3: ASTM E 84", NBSIR 82-2564, Nat. Bur. Stand.

Quintiere, J. (1982). "An Assessment of Correlations Between Laboratory and Full-Scale Experiments for the FAA Aircraft Fire Safety Program, Part 4: Flammability Tests", NBSIR 82-2525, Nat. Bur. Stand.

Quintiere, J., Harkleroad, M., and Walton, D. (1983). Measurement of Material Flame Spread Properties, Comb. Sci. Technol. 32, pp. 67-89.

Quintiere, J.G. and Harkleroad, M. (1984). "New Concepts for Measuring Flame Spread Properties", Symp. on Application of Fire Science to Fire Engineering, Amer. Soc. Testing and Materials/Soc. Fire Prot. Engrs., Denver.

Quintiere, J. (1985). "Some Factors Influencing the Fire Spread over Room Linings and in the ASTM E 84 Tunnel Test", Fire and Materials.

Saito, K., Williams, F.A. Quintieres, J. (1984). Upward Turbulant Flame spread, (to be published).

Sarkos, C.P., Hill, R.G. and Howell, W.D. (1982). "The Development and Application of a Full-Scale Wide Body Test Article to Study the Behavior of Interior Materials During a Postcrash Fuel Fire", AGARD, Aircraft Fire Safety Lecture Series No. 123, France, NATO.

Sibulkin, M. and Kim, J. (1977). Comb. Sci. and Technol., Vol. 17, pp. 39-49.

Smith, E.E. and Satija, S. (1981). "Release Rate Model for Developing Fires", Amer. Soc. of Mech. Engrs., ASME Paper No. 81-HT-4.

Sparrow, E.M. and Cess, R.D. (1978). Radiation Heat Transfer, Hemisphere Pub. Co./McGraw Hill Book Co.

Steckler, K.D. (1983). "Calculations of Wall Fire Spread in an Enclosure", Nat. Bur. Stand., NBSIR 83-2765.

Tamanini, F. (1977). Combustion and Flame, Vol. 30, pp. 85-101.

Tamanini, F. (1979). Seventeenth Symp. (Int.) on Combustion, The Combustion Institute, p. 1075.

Tewarson, A. (1980). "Physico-Chemical and Combustion/Pyrolysis Properties of Polymetic Materials", NBS-GCR-80-295, Nat. Bur. Stand.

Walton, W.D. and Twilley, W.H. (1984). "Heat Release and Mass Loss Rate Measurements for Selected Materials", NBSIR 84-2960, Nat. Bur. Stand.

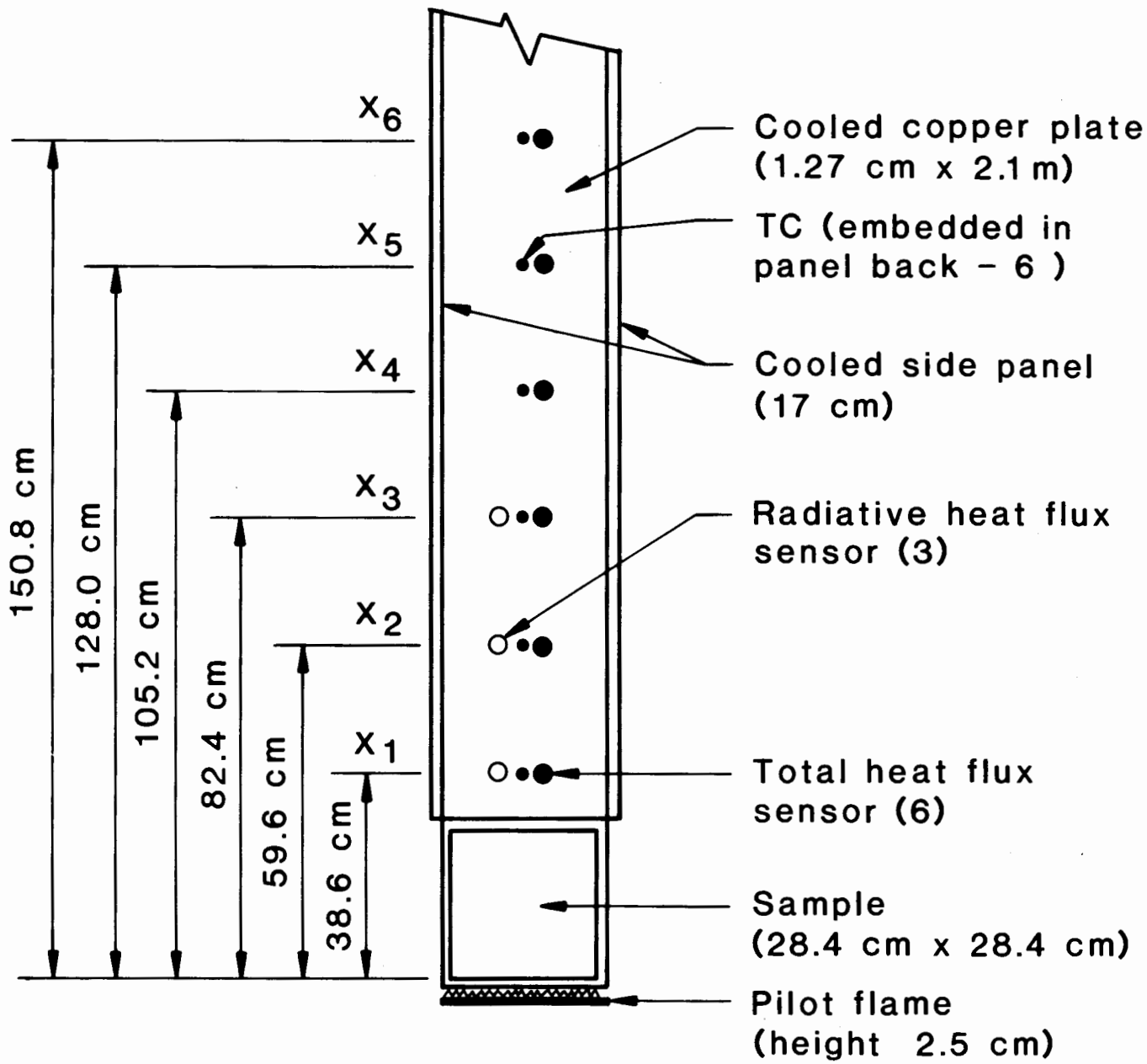

FIGURE 1. SCHEMATIC OF APPARATUS

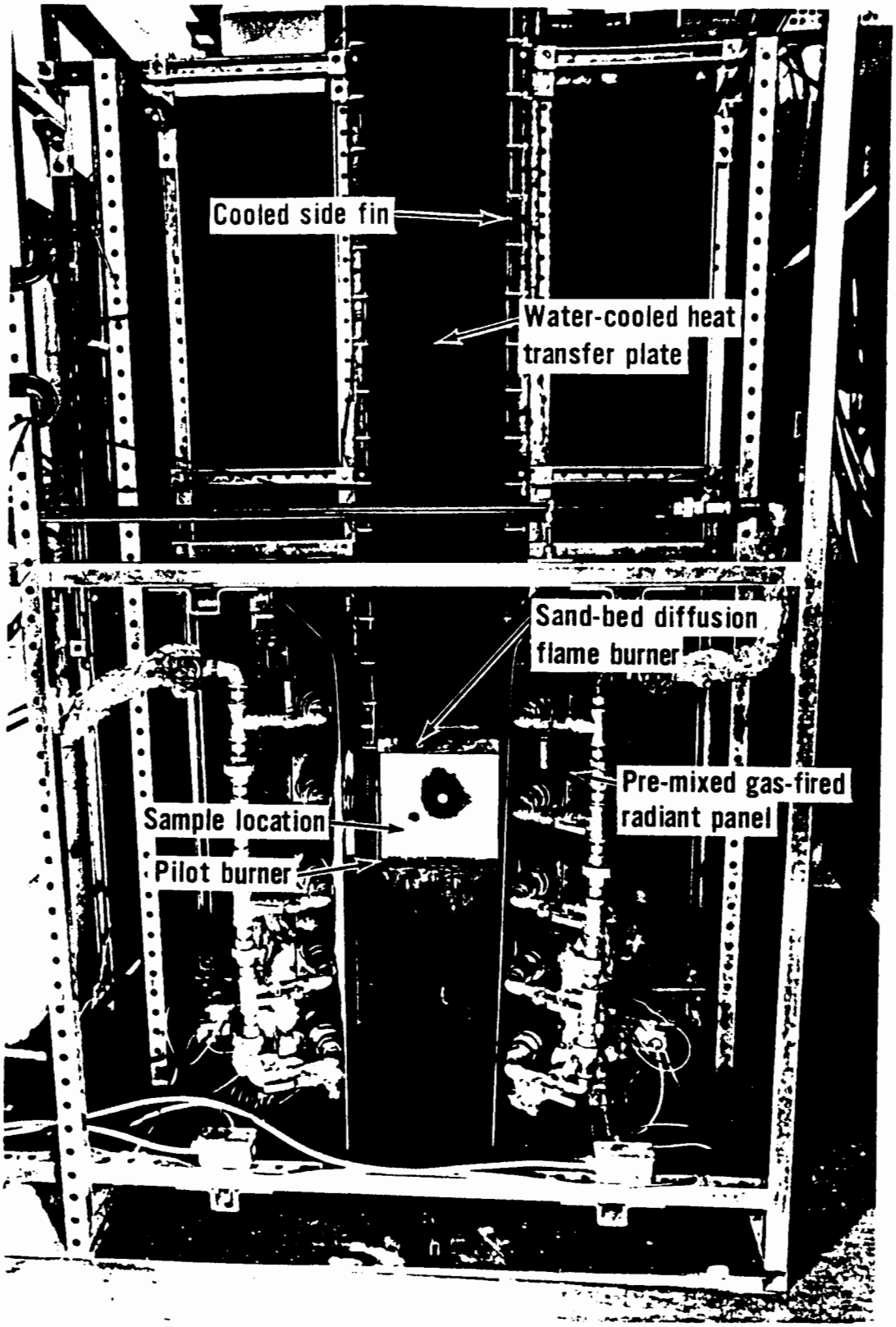

FIGURE 2. PHOTOGRAPH OF APPARATUS

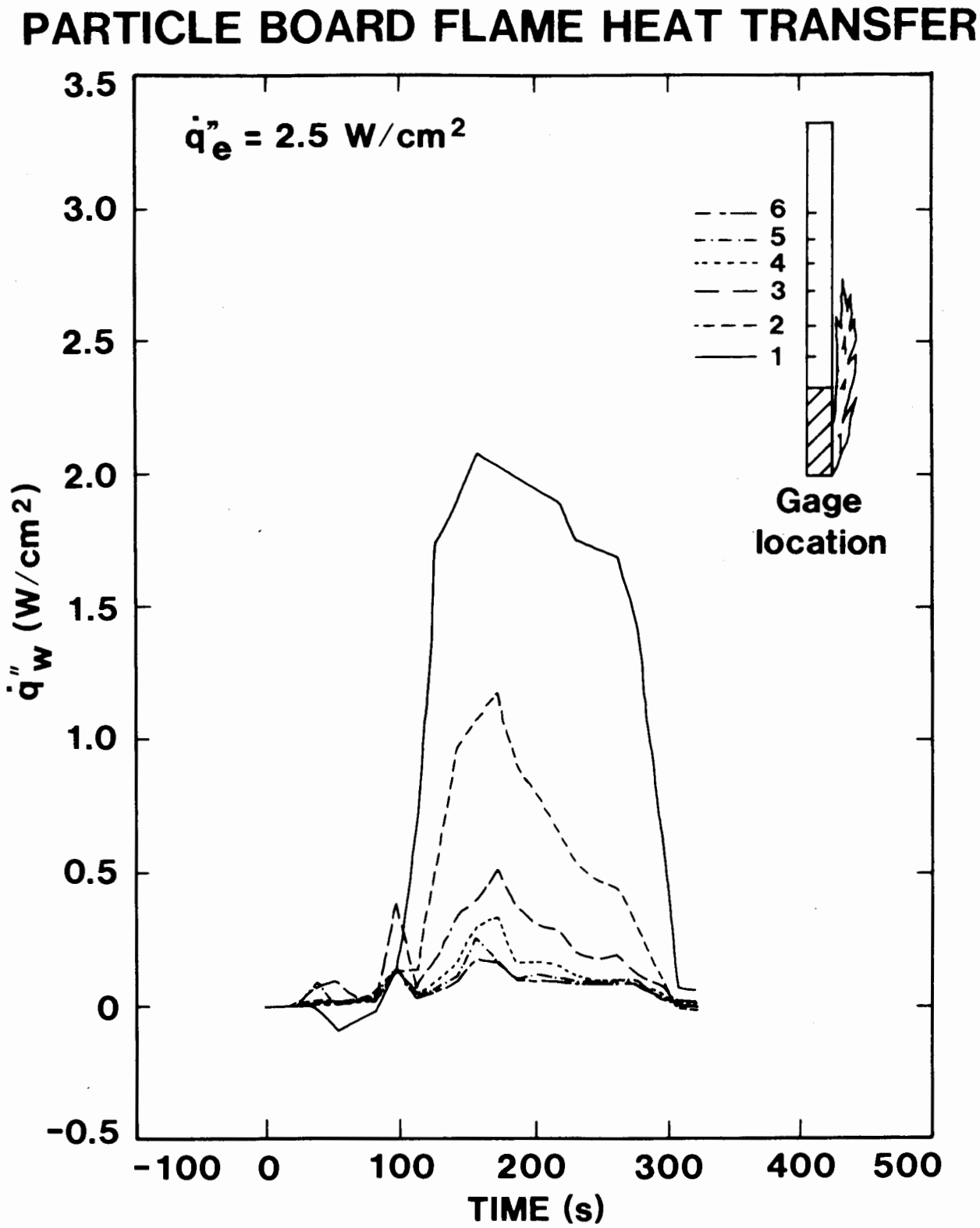

FIGURE 3. WALL HEAT FLUX FOR PARTICLE BOARD IRRADIATED AT 2.5 W/cm^2 WHERE TIME = 0 CORRESPONDS TO THE INSERTION OF THE SAMPLE.

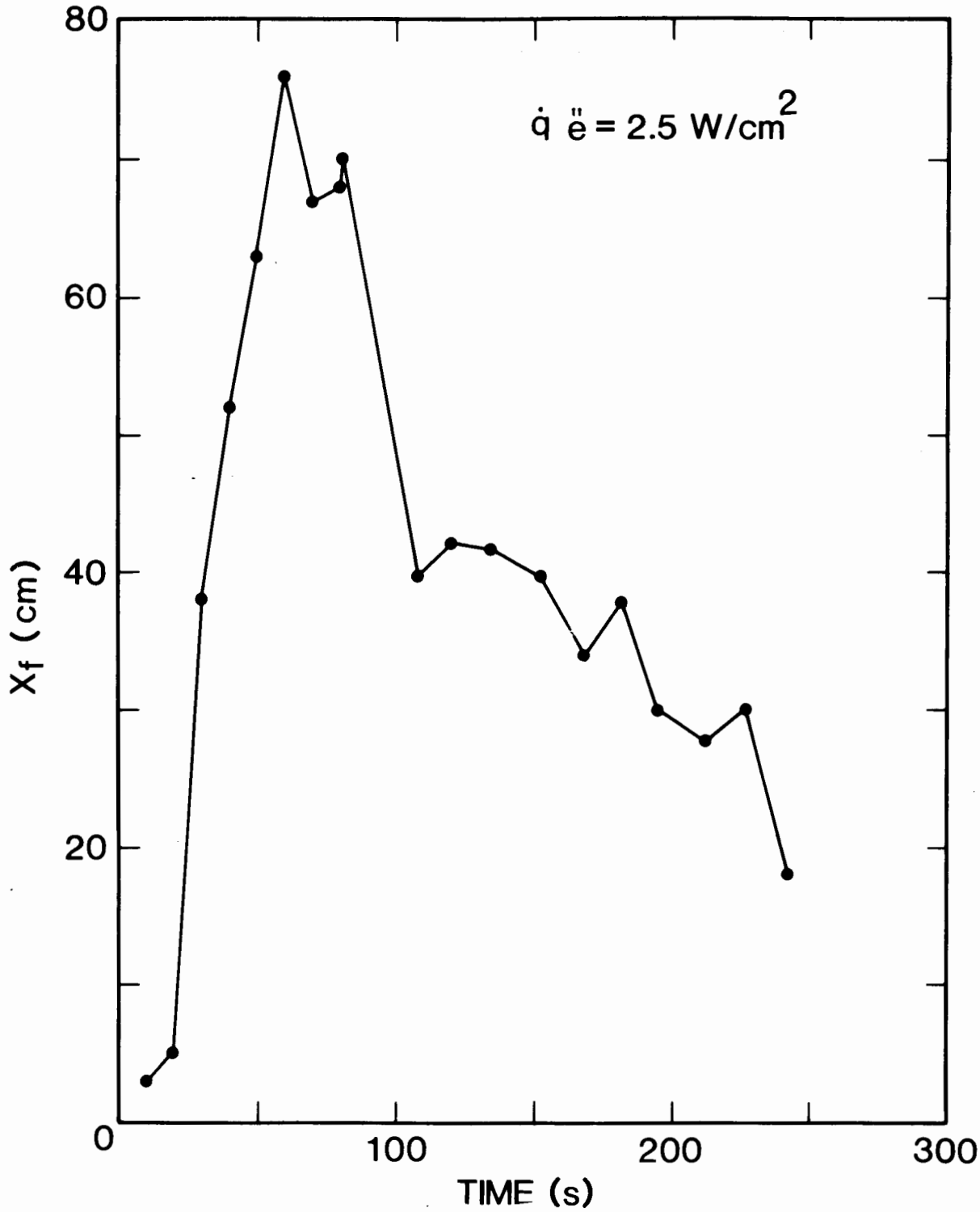

FIGURE 4. FLAME HEIGHT (TO TIPS) FOR PARTICLE BOARD IRRADIATED AT 2.5 W/cm^2 WHERE TIME = 0 CORRESPONDS TO THE IGNITION OF THE SAMPLE.

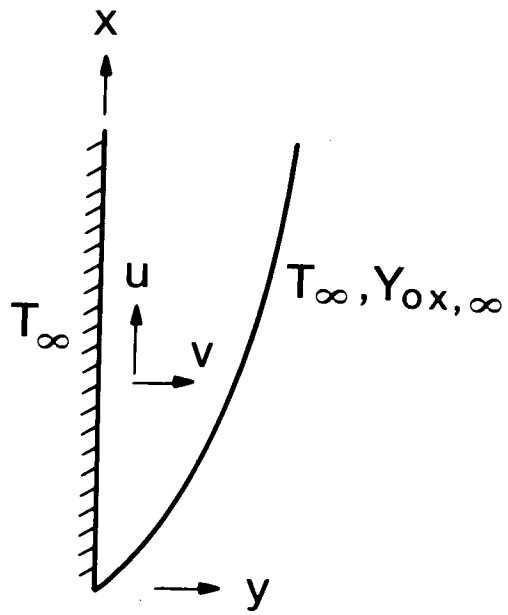

FIGURE 5. COMBUSTING BOUNDARY LAYER PROBLEM

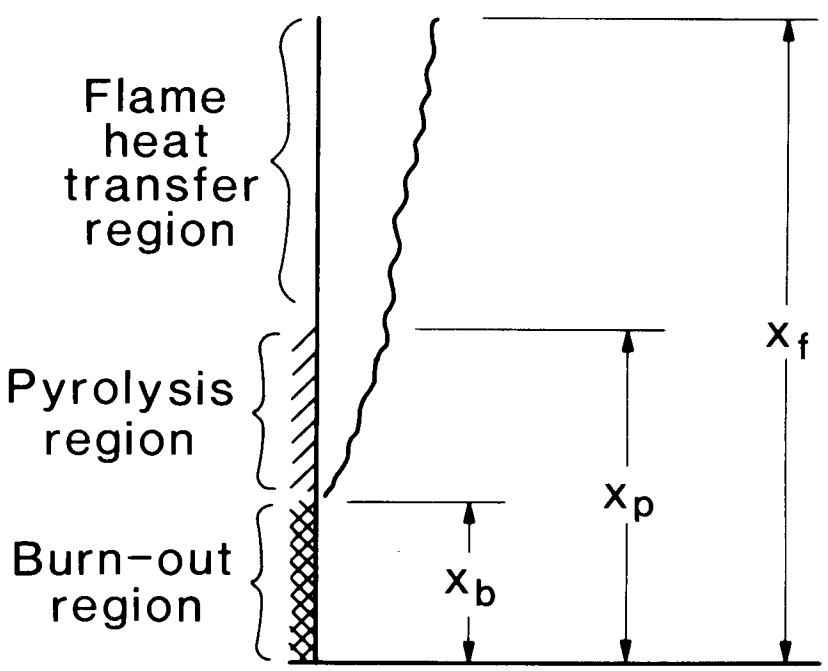

FIGURE 6. FLAME SPREAD PROBLEM

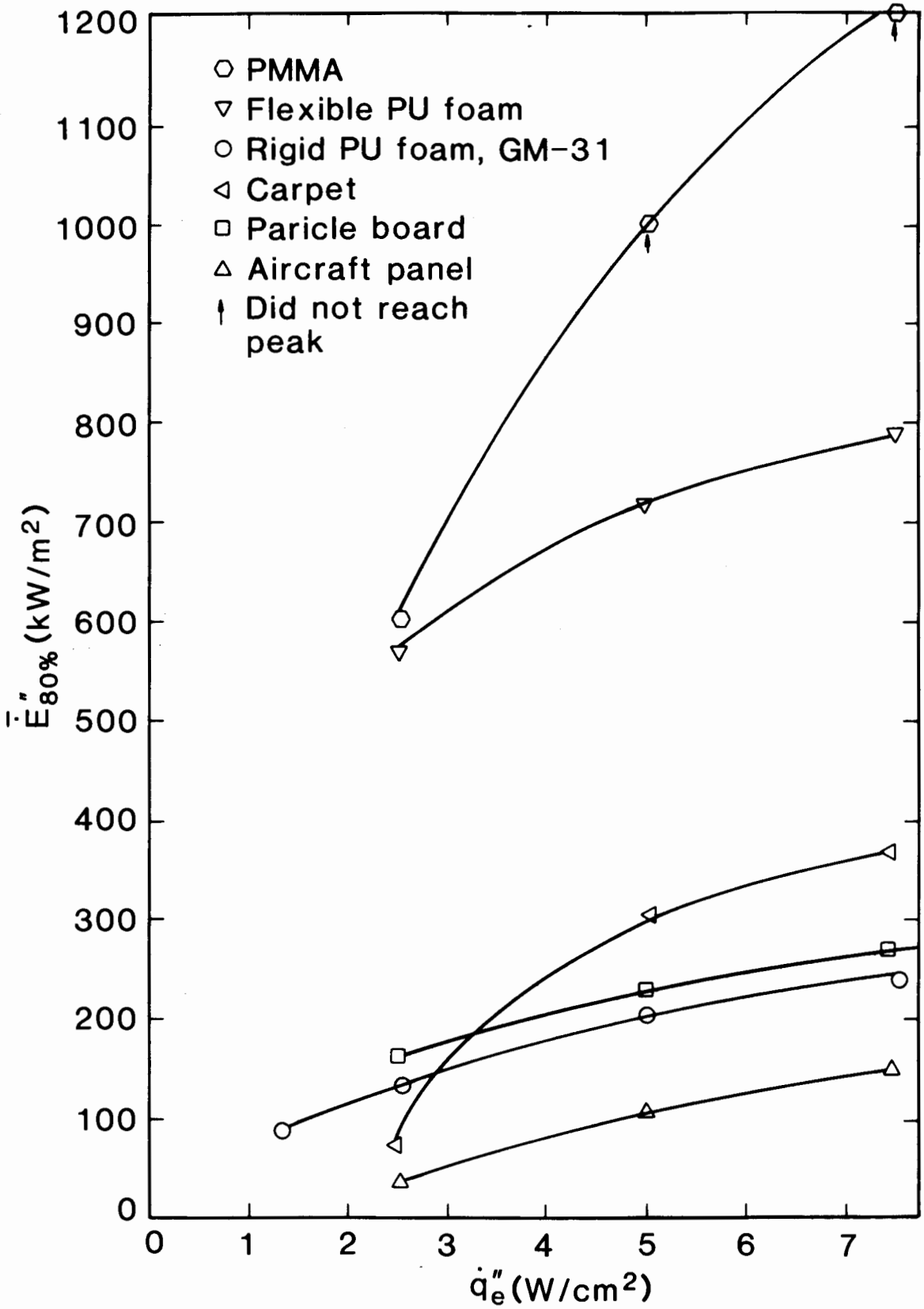

FIGURE 7. PEAK ENERGY RELEASE RATES [1].

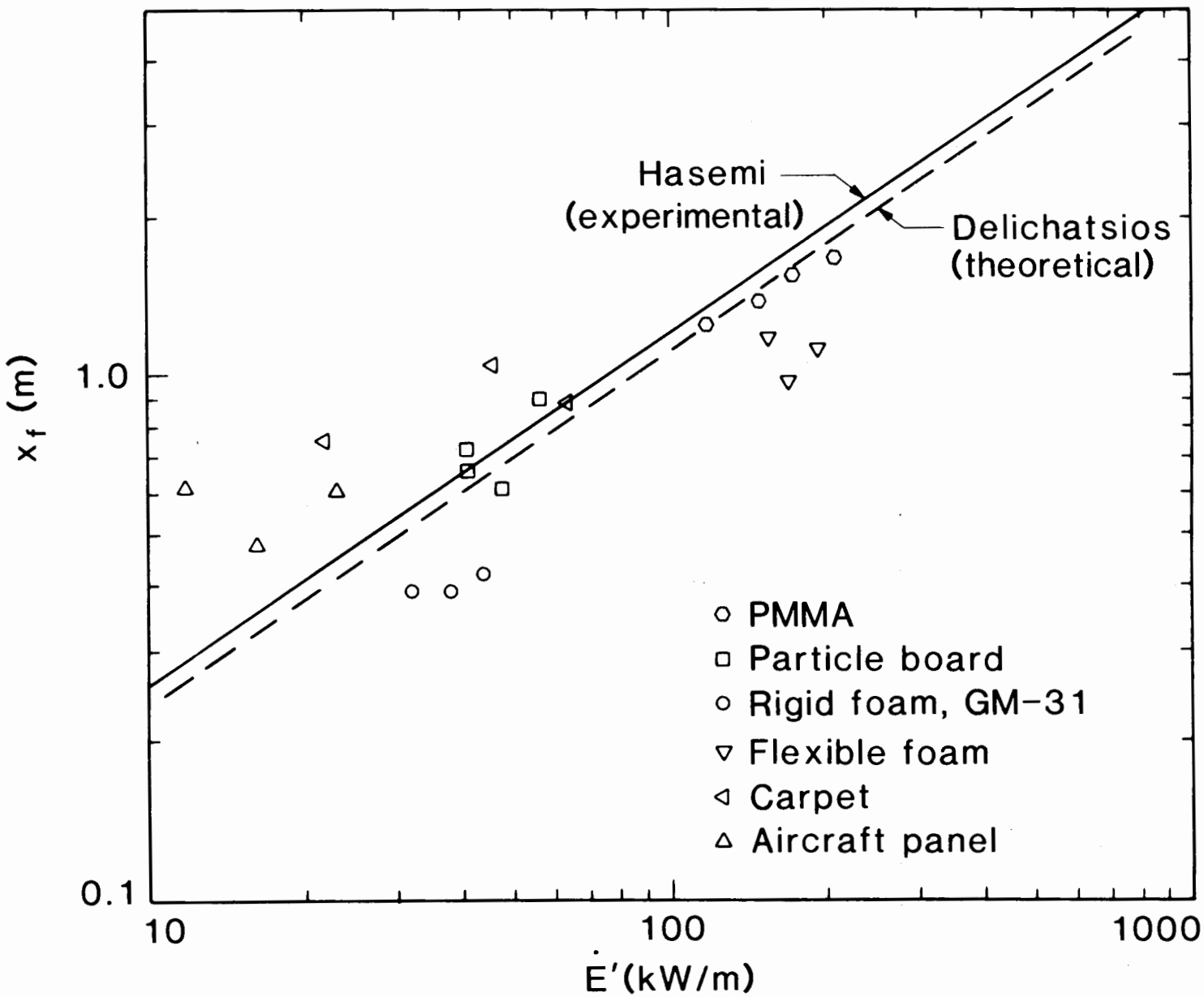

FIGURE 8. FLAME HEIGHT CORRELATION

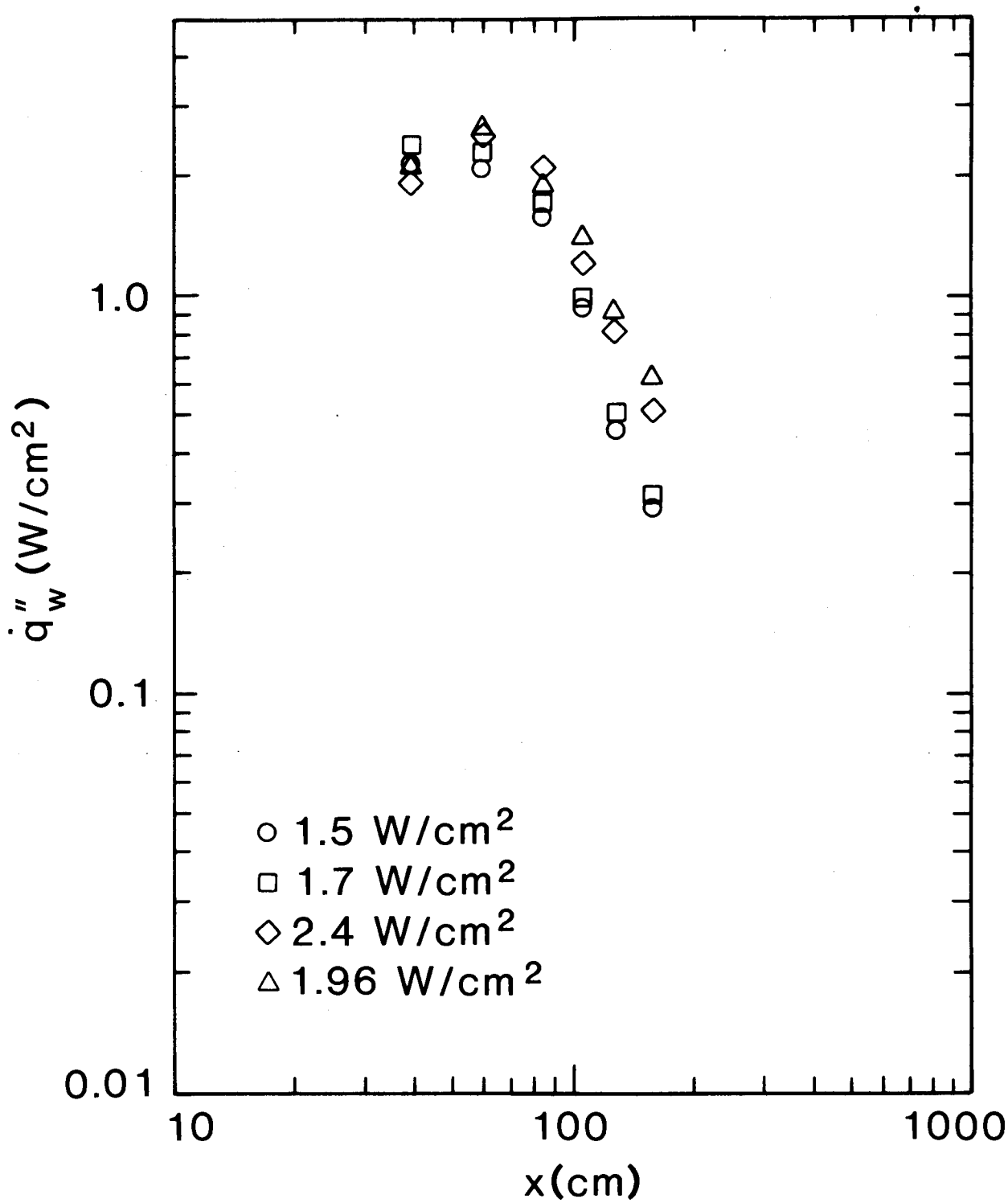

FIGURE 9A. WALL HEAT FLUX DISTRIBUTION - PMMA.

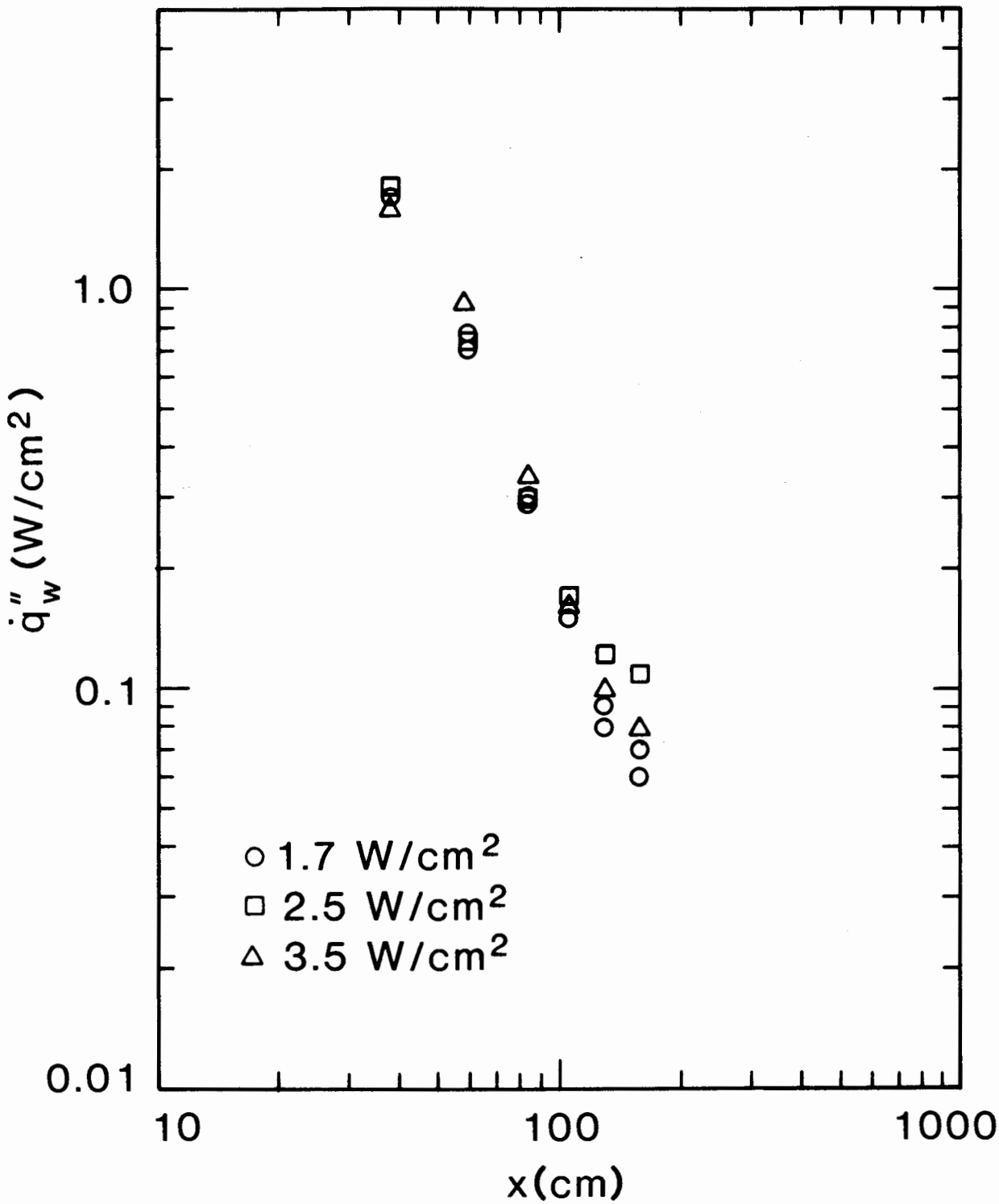

FIGURE 9B. WALL HEAT FLUX DISTRIBUTION - PARTICLE BOARD.

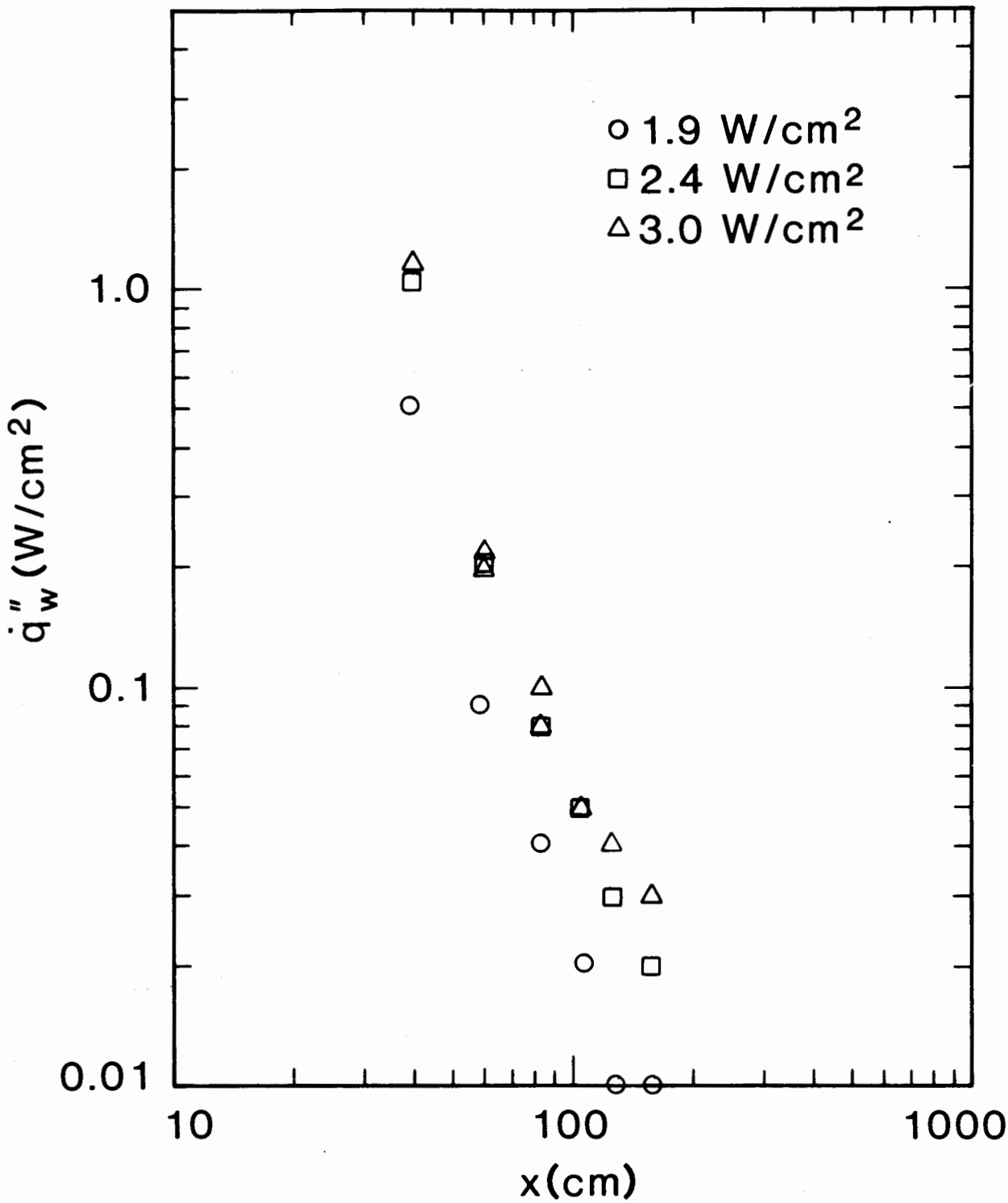

FIGURE 9C. WALL HEAT FLUX DISTRIBUTION - RIGID FOAM.

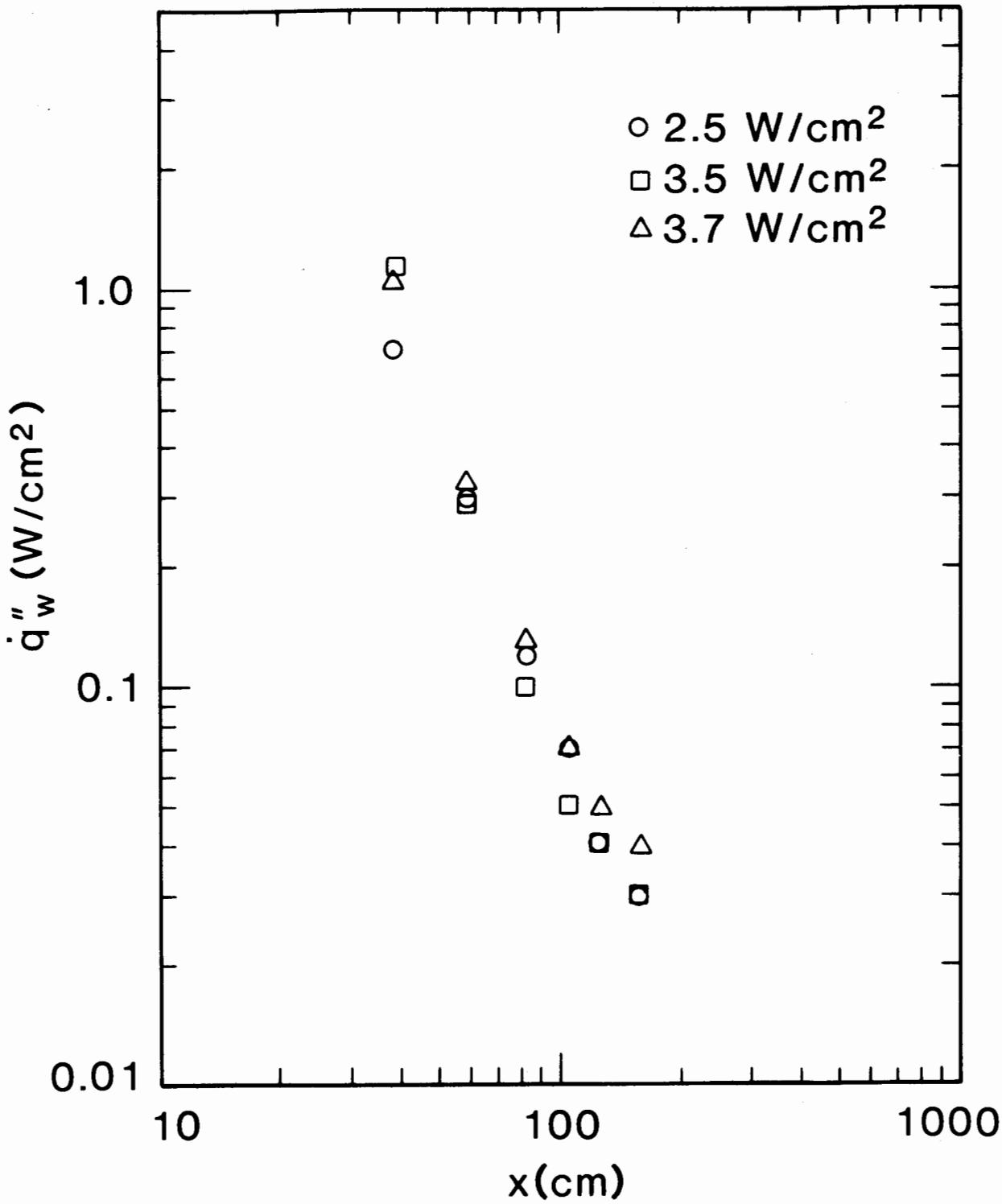

FIGURE 9D. WALL HEAT FLUX DISTRIBUTION - FLEXIBLE FOAM.

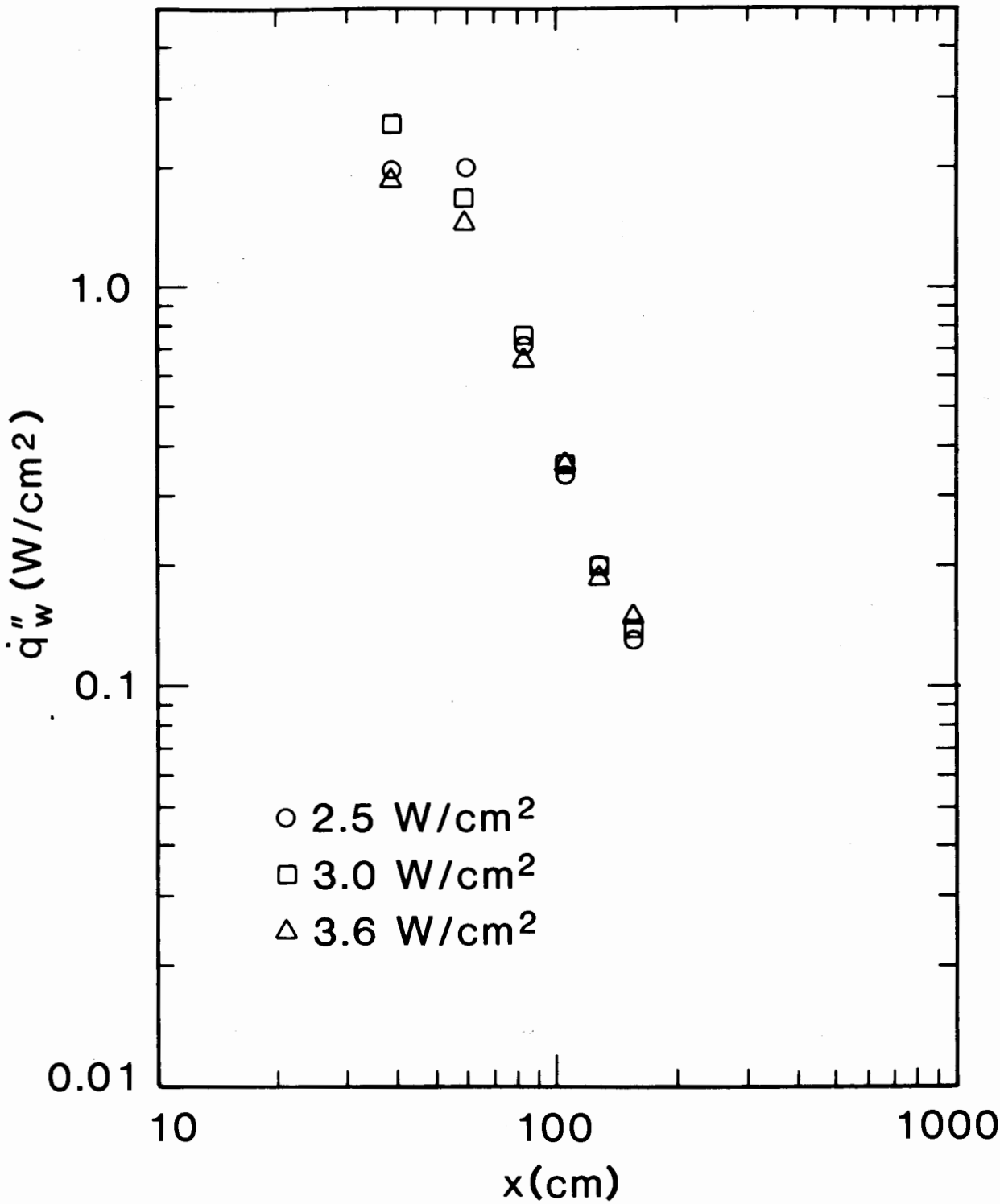

FIGURE 9E. WALL HEAT FLUX DISTRIBUTION - CARPET.

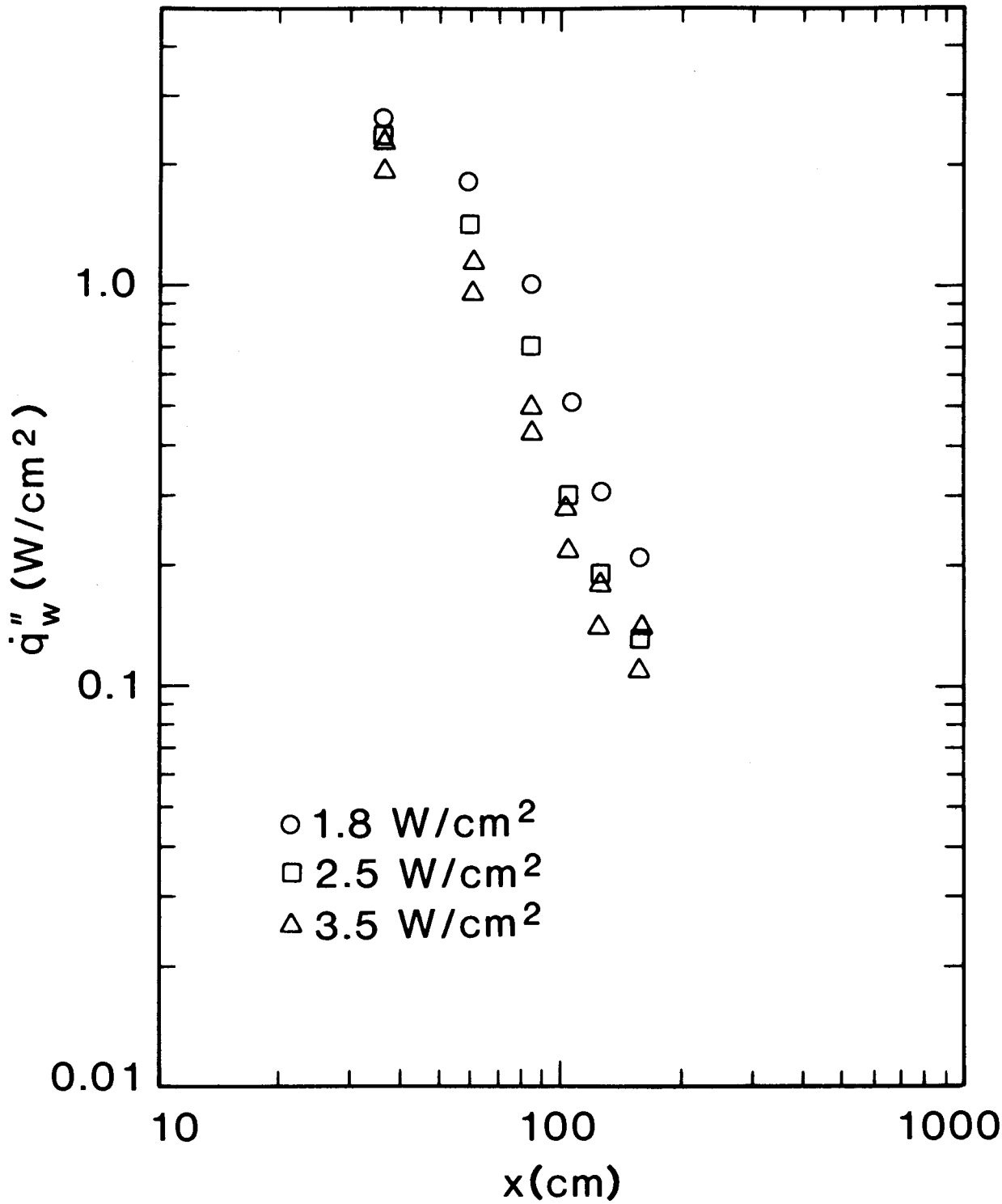

FIGURE 9F. WALL HEAT FLUX DISTRIBUTION - AIRCRAFT PANEL.

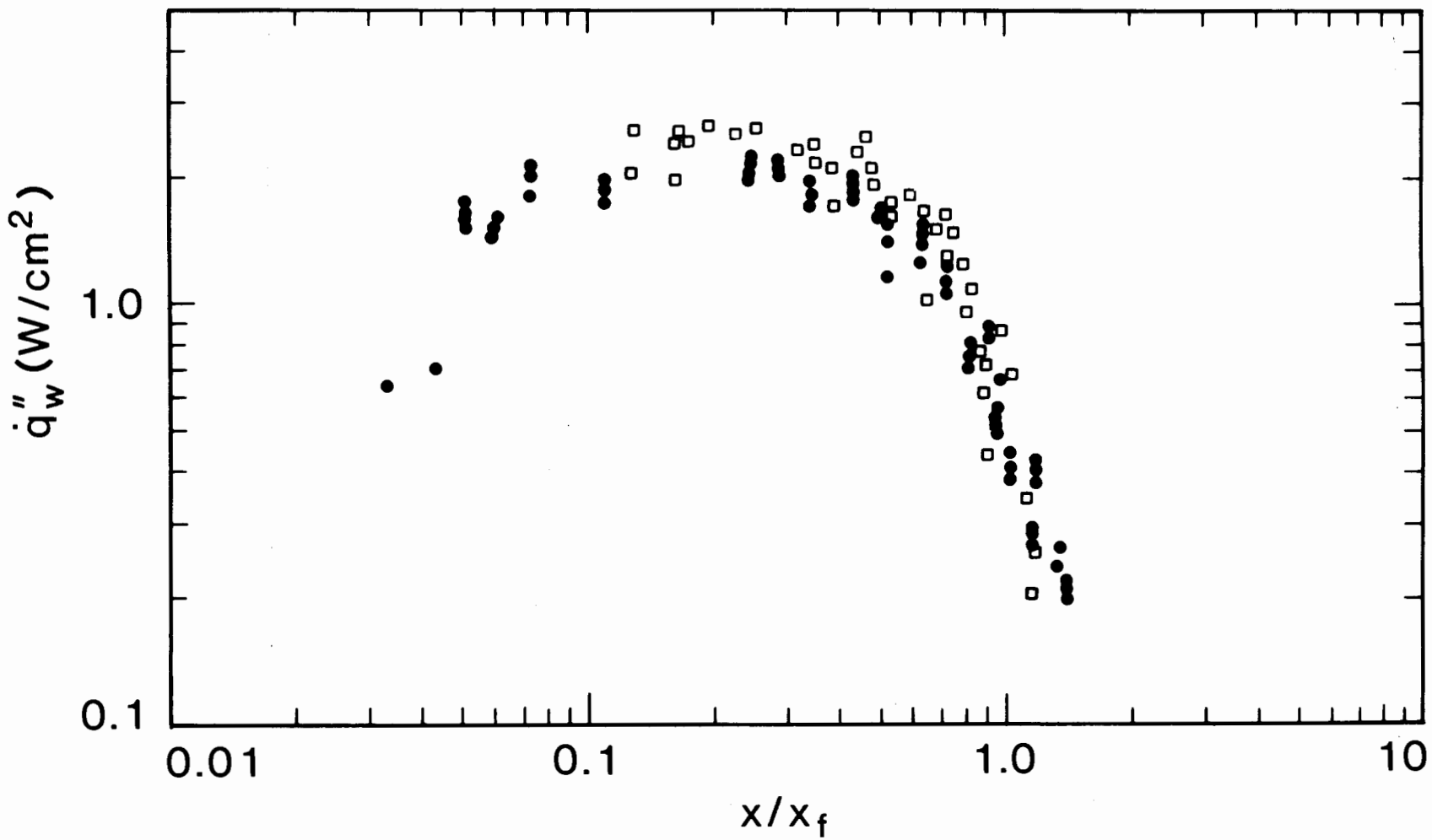

FIGURE 10. WALL HEAT FLUX FOR STEADY WALL FIRES CORRELATED WITH FLAME HEIGHT.
• CH_4 LINE BURNER FLAMES [15], □LIQUID SATURATED WALL FALMES [16]

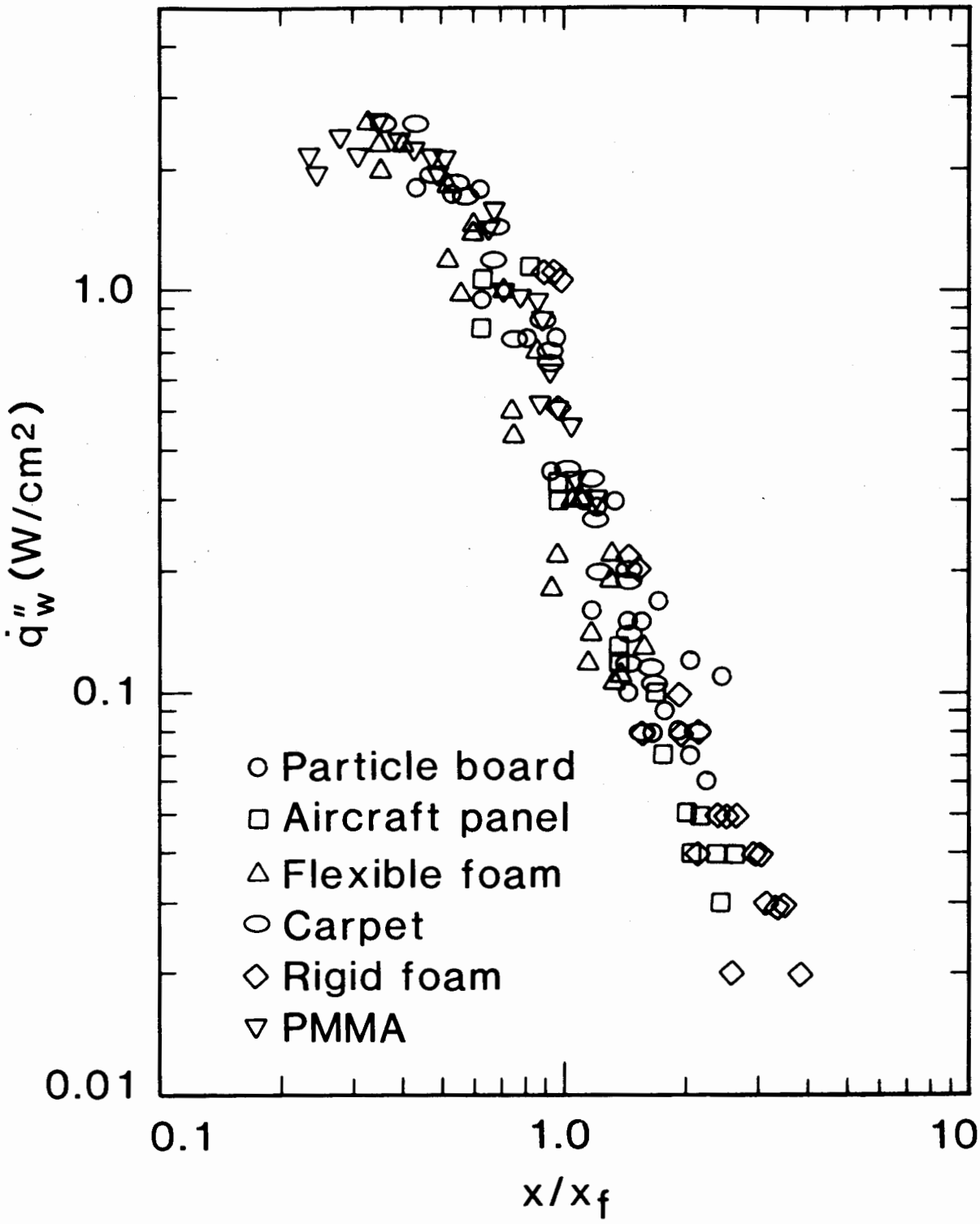

FIGURE 11. WALL HEAT FLUX CORRELATED USING FLAME HEIGHT.

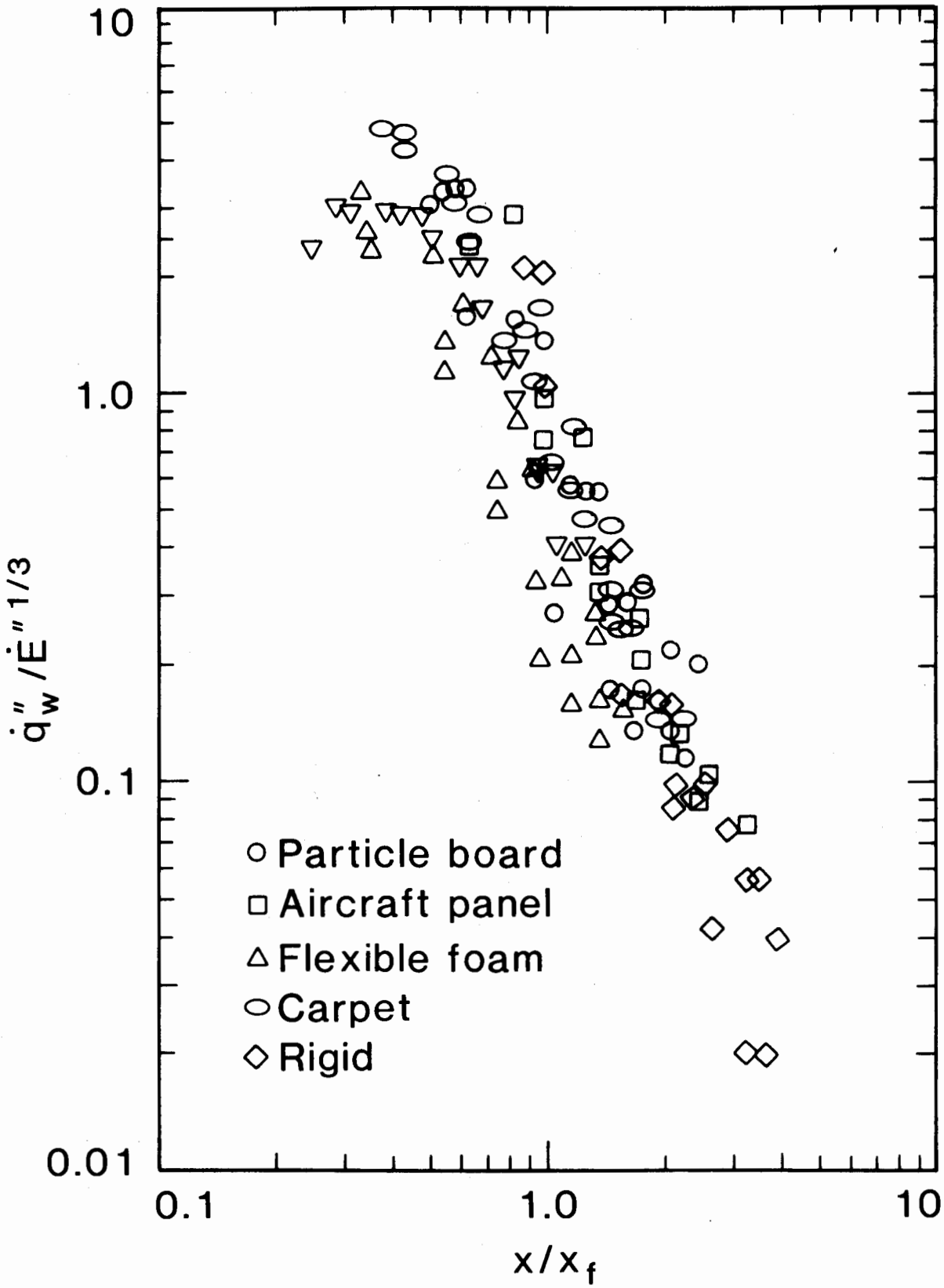

FIGURE 12. WALL HEAT FLUX CORRELATED USING FLAME HEIGHT AND ENERGY RELEASE RATE.

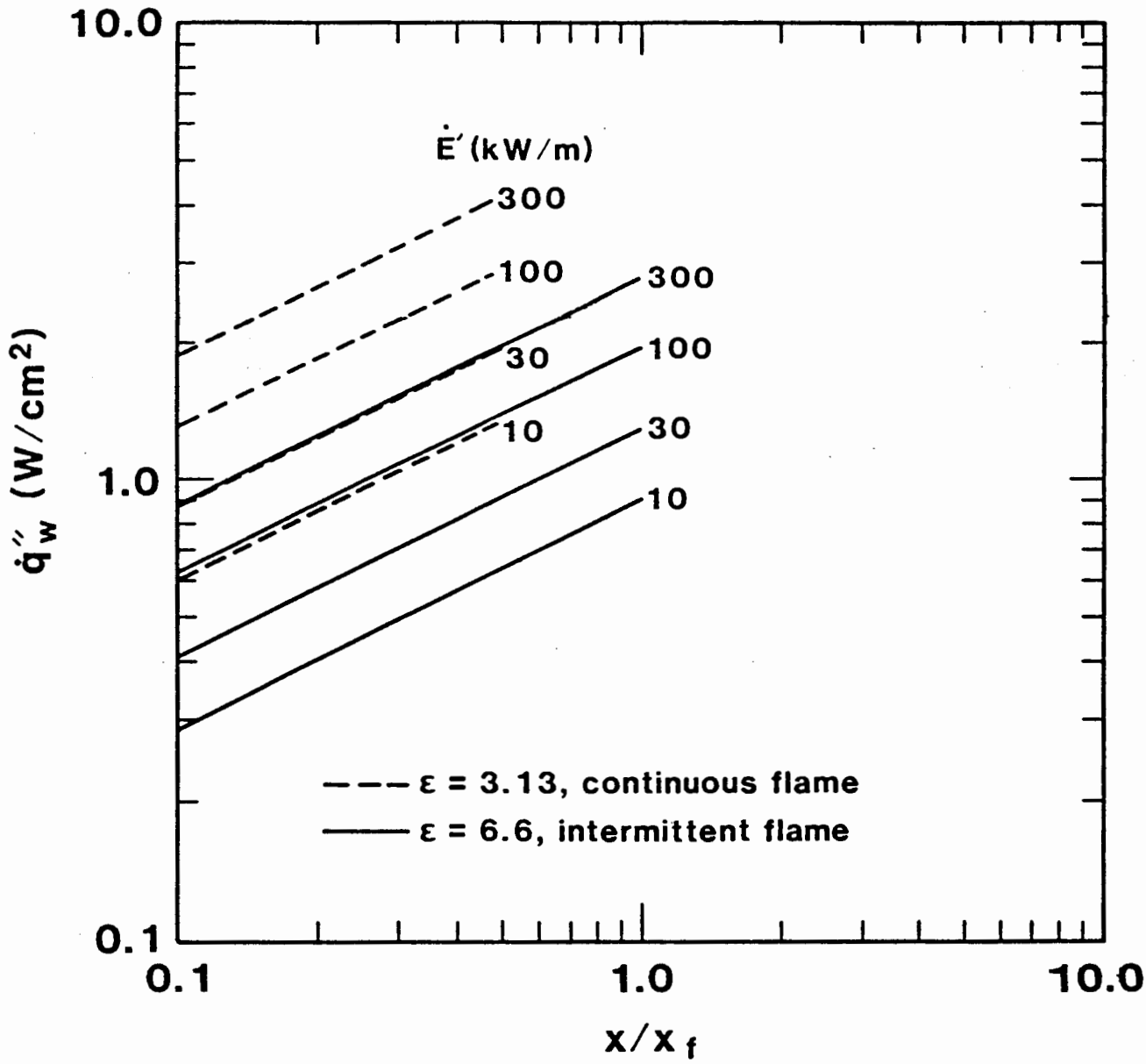

FIGURE 13. THEORETICAL WALL HEAT FLUX RESULTS FOR χ_r = 0.2.

APPENDIX A

CONVECTIVE HEATING EFFECTS ON A THIN FOIL HEAT FLUX SENSOR

The sensor was a circular foil heat flux gage of the type described by Gardon (1953). It consists of a thin constantan foil of radius R and thickness S, and was purchased commercially. The exposed surface is blackened and had an emissivity of approximately 0.98 in this case. The body and therefore the edge of the foil was maintained at a cool temperature (T_w) by water flow.

To estimate the effect of convective heat transfer the following assumptions and analysis were made.

1. No heat losses from the back face of the foil.
2. No reradiation from the front face of the foil.
3. Uniform irradiance $\dot{q}_e''$, gas temperature T_∞, and convective heat transfer coefficient h are assumed.

The governing equation for the foil heat transfer is

$$\frac{d}{dr} \; r \frac{d\phi}{dr} - m^2 r\phi = 0 \qquad \text{(A-1)}$$

$$r = R, \phi = T_w - T_\infty - \dot{q}_e''/h$$

$$r = 0, \frac{d\phi}{dr} = 0$$

where $\phi = T - T_\infty - \dot{q}_e''/h$

$m = \sqrt{h/kS}$

k = thermal conductivity of the foil.

The response of a thermocouple measuring the foil center to edge temperature difference is related to the heat flux by

$$T(0) - T_w = \left[\dot{q}_e'' + h\left(T_\infty - T_w\right)\right] \frac{1 - 1/I_o(mR)}{h} \qquad \text{(A-2)}$$

where I_o is a Bessel function. For small mR, $I_o \sim 1 + (1/2\ mR)^2$ or

$$T(0) - T_w \cong \left[\dot{q}_e'' + h\left(T_\infty - T_w\right)\right] \frac{m^2R^2}{4h} = \left[\dot{q}_e'' + h\left(T_\infty - T_w\right)\right] \frac{R^2}{4kS} \qquad \text{(A-3)}$$

Equation A-3 is equivalent to the pure radiation results in which $h \equiv 0$, and also under conditions of mR small, convection is directly additive. Moreover

the calibration constant of the sensor is not dependent on its calibration technique or its application with respect to convective or radiative heating provided mR is small, or h does not vary significantly for the conditions of calibration and application.

The values of mR for the sensors used, with $h = 7\ W/m^2K$ determined in calibration with a radiant source and hot water (47°C), can be computed as follows:

$$R = 0.217\ cm = 2.17 \times 10^{-3}\ m,$$
$$S = 0.0025\ cm = 2.5 \times 10^{-5}\ m,$$
$$k = 21.6\ W/m^2K,$$

and mR = 0.25. This is small enough for Eq. A-3 to hold with good accuracy. Moreover, under the natural convection conditions of this experiment, it is not expected that h will vary markedly.

APPENDIX B

RADIATIVE ANALYSIS FOR A HOMOGENEOUS WALL FLAME

For a non-uniform temperature wall flame represented as a constant thickness slab, infinite in extent with the wall and ambient temperatures equal to T_o, it can be shown (Sparrow and Cess, 1978) that the radiative flux is given as

$$\dot{q}_r''(y) = 2\left\{B_1E_3(\tau) - B_2E_3(\tau_o - \tau) + \int_o^{\tau} \sigma T^4 E_2(\tau - t)\,dt - \int_{\tau}^{\tau_o} \sigma T^4 E_2(t-\tau)dt\right\} \quad \text{(B-1)}$$

where E_2 and E_3 are exponential integral functions. The position y is measured from the wall, B_1 and B_2 are the bounding surface radiosities both equal to σT_o^4, and

$$\tau = \int_o^y \kappa dy \quad \text{(B-2)}$$

$$\tau_o = \int_o^{\delta} \kappa dy \quad \text{(B-3)}$$

with κ the absorption coefficient of the flame and δ is its thickness.

The wall flux (y=0) for $\tau_o \ll 1$, i.e., optically thin, can be written as

$$\dot{q}_{r,w}'' = 2\int_o^{\tau_o} \sigma T^4 dt + 2\tau_o\,\sigma T_o^4 \quad \text{(B-4)}$$

since $E_3 \sim 1/2 - \tau$ and $E_2 \sim 1$. In this case the last term is small and may also be dropped. An identical expression results for the flux at the free boundary interface, which implies that the flame radiation splits equally in both directions.

☆U.S. GOVERNMENT PRINTING OFFICE: 1985—505-080/20094